Cellular/Molecular

Calcium-Regulation of Mitochondrial Respiration Maintains ATP Homeostasis and Requires ARALAR/AGC1-Malate Aspartate Shuttle in Intact Cortical Neurons

Irene Llorente-Folch,[1,2]* Carlos B. Rueda,[1,2]* Ignacio Amigo,[1,2] Araceli del Arco,[2,3] Takeyori Saheki,[4] Beatriz Pardo,[1,2] and Jorgina Satrústegui[1,2]

[1]Departament of Molecular Biology, Centre for Molecular Biology Severo Ochoa UAM-CSIC, Autonomous University of Madrid, Madrid, Spain, [2]CIBER or Rare Diseases (CIBERER), [3]Area of Biochemistry, Regional Centre for Biochemical Research (CRIB), Faculty of Environmental Science and Biochemistry, University of Castilla-La Mancha, Toledo Spain, and [4]Institute of Resource Development and Analysis, Kumamoto University, Honjo, Kumamoto, Japan

Neuronal respiration is controlled by ATP demand and Ca^{2+} but the roles played by each are unknown, as any Ca^{2+} signal also impacts on ATP demand. Ca^{2+} can control mitochondrial function through Ca^{2+}-regulated mitochondrial carriers, the aspartate-glutamate and ATP-Mg/Pi carriers, ARALAR/AGC1 and SCaMC-3, respectively, or in the matrix after Ca^{2+} transport through the Ca^{2+} uniporter. We have studied the role of Ca^{2+} signaling in the regulation of mitochondrial respiration in intact mouse cortical neurons in basal conditions and in response to increased workload caused by increases in $[Na^+]_{cyt}$ (veratridine, high-K^+ depolarization) and/or $[Ca^{2+}]_{cyt}$ (carbachol). Respiration in nonstimulated neurons on 2.5–5 mM glucose depends on ARALAR-malate aspartate shuttle (MAS), with a 46% drop in *aralar* KO neurons. All stimulation conditions induced increased OCR (oxygen consumption rate) in the presence of Ca^{2+}, which was prevented by BAPTA-AM loading (to preserve the workload), or in Ca^{2+}-free medium (which also lowers cell workload). SCaMC-3 limits respiration only in response to high workloads and robust Ca^{2+} signals. In every condition tested Ca^{2+} activation of ARALAR-MAS was required to fully stimulate coupled respiration by promoting pyruvate entry into mitochondria. In *aralar* KO neurons, respiration was stimulated by veratridine, but not by KCl or carbachol, indicating that the Ca^{2+} uniporter pathway played a role in the first, but not in the second condition, even though KCl caused an increase in $[Ca^{2+}]_{mit}$. The results suggest a requirement for ARALAR-MAS in priming pyruvate entry in mitochondria as a step needed to activate respiration by Ca^{2+} in response to moderate workloads.

Introduction

Oxygen consumption is controlled by the mitochondrial proton electrochemical gradient ($\Delta\mu H^+$; Mitchell and Moyle, 1969). In most cell types, $\Delta\mu H^+$ is mainly used in ATP synthesis. Increases in cell workload will consume ATP and lead to increased ATP production in mitochondria, through the utilization of $\Delta\mu H^+$. This in turn, will stimulate respiration. However, even at high workloads, a rapid formation of ATP through phosphocreatine and the creatine kinase reaction maintains cell ATP at almost constant levels (Cerdan et al., 1990).

In excitable cells, Ca^{2+} regulates cell function both by activation of ATP consumption (contraction, ion transport) and by activating ATP production through stimulation of oxidative phosphorylation. Ca^{2+} regulation of oxidative phosphorylation is thought to involve Ca^{2+} entry in mitochondria through the Ca^{2+} uniporter (MCU) and activation of three matrix dehydrogenases and complex V (McCormack et al., 1990; Glancy and Balaban, 2012). It may also occur through Ca^{2+} activation of mitochondrial metabolite transporters, by Ca^{2+} acting on the external side of the inner mitochondrial membrane. There are two types of such transporters, the aspartate-glutamate carriers (AGCs) and the ATP-Mg/Pi transporters (del Arco and Satrústegui, 1998; Palmieri et al., 2001; Satrústegui et al., 2007; Traba et al., 2012; Amigo et al., 2013).

ARALAR/AGC1 is present in brain and it is a component of the malate aspartate NADH shuttle (MAS). Activation by extramitochondrial Ca^{2+} of ARALAR-MAS results in an increase in NADH production in neuronal mitochondria (Pardo et al., 2006) and Gellerich et al. (2009, 2012, 2013) have proposed that Ca^{2+}-activation of ARALAR functions as a "gas pedal" to increase pyruvate formation.

SCaMC-3 is the main mitochondrial ATP-Mg/Pi carrier present in brain and liver (del Arco and Satrústegui, 2004;

Received March 1, 2013; revised June 11, 2013; accepted June 13, 2013.

Author contributions: I.L.-F., C.B.R., A.d.A., B.P., and J.S. designed research; I.L.-F. and C.B.R. performed research; T.S. contributed unpublished reagents/analytic tools; I.L.-F., C.B.R., and I.A. analyzed data; I.L.-F., C.B.R., and J.S. wrote the paper.

This work was supported by the Ministerio de Economía Grant BFU2011-30456, by CIBERER (an initiative of the ISCIII), by the Comunidad de Madrid Grant S2010/BMD-2402 MITOLAB-CM (to J.S.), by ISCIII Grant PI080610 (to A.d.A.), and by an institutional grant from the Fundación Ramon Areces to the Centro de Biología Molecular Severo Ochoa. C.B.R is a recipient of a FPU fellowship from the Ministerio de Educación y Ciencia. We thank Dr. Hiromi Imamura, Kyoto University for kindly providing the GO-ATeam plasmids. We thank Isabel Manso, Alejandro Arandilla, and Bárbara Sesé for technical support, José Belio for his help in preparing the figures, and María Angeles Muñoz, from the Unit of Optical and Confocal Microscopy, for her inestimable support.

The authors declare no competing financial interests.

*I.L.-F. and C.B.R. contributed equally to this work.

Correspondence should be addressed to Dr. Jorgina Satrústegui, Universidad Autonoma de Madrid, Centro de Biologia Molecular Severo, Nicolas Cabrera 1, Madrid, 28049, Spain. E-mail: jsatrustegui@cbm.uam.es.

DOI:10.1523/JNEUROSCI.0929-13.2013

Fiermonte et al., 2004; Amigo et al., 2013). Although not involved in oxidative phosphorylation, which requires adenine nucleotide exchange by the ADP/ATP carriers, adenine nucleotide accumulation in rat liver mitochondria through the ATP-Mg/Pi carrier results in a progressive increase in state 3 respiration (ADP-stimulated respiration; Asimakis and Aprille, 1980; Aprille et al., 1987; Amigo et al., 2013), perhaps by increasing the driving force of the ATP-synthase (Balaban et al., 2009; Glancy and Balaban, 2012).

The control of respiration by Ca^{2+} in intact neurons is still largely unknown. Hayakawa et al. (2005) described rapid Ca^{2+}-dependent changes in oxygen consumption in response to high KCl in cultured Purkinje neurons, but Mathiesen et al. (2011) found no evidence for a role of cytosolic Ca^{2+} in activity-dependent rises in cerebral metabolic rate of oxygen ($CMRO_2$) in cerebellar Purkinje neurons in the intact brain. Bak et al. (2012) described a Ca^{2+}-induced increased in flux through the tricarboxylic acid cycle in cerebellar neurons using glucose as substrate. A confounding variable in these and other studies relates to the coincidence of the Ca^{2+}-mechanism with the classical mechanism activating mitochondrial respiration, i.e., ATP demand. Indeed, any Ca^{2+} signal involves ATP consumption to recover prestimulation values, and the role of Ca^{2+} versus ADP-stimulation of respiration needs to be established.

The purpose of this work was to study the role of Ca^{2+} in the control of respiration under basal conditions and in response to an increase in workload in neuronal cultures. Particularly, to evaluate the contribution of the ARALAR-MAS and SCaMC-3 pathways of Ca^{2+} signaling to mitochondria with respect to that of MCU.

Materials and Methods

Animals. Male SVJ129 × C57BL/6 mice carrying a deficiency for *aralar* expression (*aralar* $^{-/-}$, *aralar* $^{+/-}$, and *aralar* $^{+/+}$) obtained from Lexicon Pharmaceuticals were used (Jalil et al., 2005). Mice deficient in SCaMC-3 were generated by Lexicon Pharmaceuticals with a mixed C57BL6/Sv129 genetic background (Amigo et al., 2013). Animals are born in Mendelian proportions and show no evident phenotypic traits. The mice were housed in a humidity- and temperature-controlled room on a 12 h light/dark cycle, receiving water and food *ad libitum*. All the experimental protocols performed in this study were performed in accordance with procedures approved in the Directive 86/609/EEC of the European Union and with approval of the local Ethics Committee of the Universidad Autónoma de Madrid. All efforts were made to minimize animal suffering.

Genotypes. Genotypes were determined, as previously described for *aralar* (Pardo et al., 2006) and *SCaMC-3* (Amigo et al., 2013), by PCR using genomic DNA obtained from tail or embryonic tissue samples (Nucleospin tissue kit, Macherey-Nagel). PCR mixtures were preincubated at 94°C for 5 min, followed by 35 cycles of DNA amplification at 94°C for 60 s, 58°C for 60 s, and 72°C for 60 s; the process was finished with incubation at 72°C for 5 min. DNA fragments were separated by electrophoresis on a 1.5% agarose gel.

Neuronal culture. Cortical neuronal cultures were prepared from E15–E16 mouse embryos as described earlier (Ramos et al., 2003; Pardo et al., 2006). Embryos were obtained from crosses between C57BL6/SV129 *aralar*$^{+/-}$ mice, C57BL6/SV129 *SCaMC-3* $^{+/+}$, or C57BL6/SV129 *SCaMC-3* $^{-/-}$ mice and nonbrain tissue was used for determination of DNA genotype. Neurons represented >80% of the total cell population (Ramos et al., 2003; Pardo et al., 2006) and included both glutamatergic and GABAergic neurons (results not shown).

Determination of glucose, lactate, and pyruvate. Glucose, lactate, and pyruvate determinations in media from neuronal cell cultures were performed as follows. Cortical neurons were cultured in 12-well plates for 10 DIV and the experiment was performed in free-serum B27-supplemented neurobasal-A medium with 5 mM glucose. Aliquots of the medium were collected at various times (up to 2 h). Lactate content was determined enzymatically (Cuezva et al., 1982; Sánchez-Cenizo et al., 2010). Glucose and pyruvate concentrations in the media were determined by using kits from Boehringer (glucose) and Instruchemie BV (pyruvate) following the manufacturer's instructions in 48-well microplates, with a FLUOstar OPTIMA reader in the absorbance mode. The consumption of glucose, pyruvate, and net formation of lactate by the cells was calculated on the basis of cellular protein. Results are mean ± SEM (n = 7–15) of two to four independent experiments. Data were statistically evaluated by one-way ANOVA followed by Student's t test. Comparisons between control and *aralar*-deficient cultures were significant where indicated $^{***}p \leq 0.001$.

Cytosolic Na^{+} and Ca^{2+} imaging in primary neuronal cultures. Neurons growing on poly-lysine-coated coverslips were loaded with 5 μM Fura-2 AM and 50 μM pluronic acid F.127 (Invitrogen) for 30 min at 37°C in Ca^{2+}-free HCSS (120 mM NaCl, 0.8 $MgCl_2$, 25 mM HEPES, 5.4 mM KCl, pH 7.4), 2.5 mM glucose, and washed for 30 min in HCSS (2 mM $CaCl_2$, 2.5 mM glucose). Then coverslips were mounted on the microscope stage equipped with a 40× objective as described previously (Ruiz et al., 1998) and Fura-2 fluorescence was imaged ratiometrically using alternate excitation at 340 and 380 nm, and a 510 nm emission filter with a Neofluar 40×/0.75 objective in an Axiovert 75M microscope (Zeiss). Additions were made as a bolus or, for isosmotic high K^{+}, changing to a "isosmotic" HCSS in which 30 mM NaCl was replaced by 30 mM KCl (90 mM NaCl, 0.8 $MgCl_2$, 25 mM HEPES, 35.4 mM KCl, pH 7.4) during continuous superfusion (≈1.5 ml/min). $[Ca^{2+}]_i$ and $[Na^{+}]_i$ imaging was performed as described with Fura-2 as Ca^{2+} indicator (Ruiz et al., 1998; Pardo et al., 2006) and sodium-binding benzofuran isophthalate (SBFI) as a sodium indicator (Rose and Ransom, 1997) at 37°C. For single-cell analysis of $[Ca^{2+}]_i$ and $[Na^{+}]_i$ the ratio of fluorescence intensity at 340 nm ($F_{(340)}$) and 380 nm ($F_{(380)}$) ($F_{(340)}/F_{(380)}$) was obtained. Signal calibration for Fura-2 $[Ca^{2+}]_i$ imaging Ca^{2+} was performed with 1 μM Br-A23 Ca^{2+} ionophore (Sigma-Aldrich), with (Rmin) or without (Rmax) preincubation with 2 mM EGTA. Neuronal fluorescence at both wavelengths was corrected for autofluorescence after digitonin-permeabilization and quenching of Fura-2 fluorescence with 4 mM $MnCl_2$. Ratio measurements were converted to Ca^{2+} concentrations as described previously (Grynkiewicz et al., 1985). Na^{+} imaging was performed as previously described (Rose and Ransom, 1997), briefly, 20 μM SBFI-AM was loaded during 90 min in the presence of 50 μM pluronic acid F.127 in HCSS 2 mM $CaCl_2$ then washed and equilibrated for another 30 min. Monensin (10 μM) and ouabain (0.1 mM) were added for equilibration of extra- and intracellular $[Na^{+}]$ at the end of the experiments. Image acquisition was performed with the Aquacosmos 2.5 software (Hamamatsu) and data analysis was done with Origin software (OriginLab). When required, BAPTA loading was performed in Ca^{2+}-free HCSS, 50 μM BAPTA-AM coloaded with Fura-2 AM during 30 min, then washed and equilibrated in HCSS 2 mM $CaCl_2$ medium for another 30 min.

Mitochondrial Ca^{+2} and cytosolic ATP imaging. To image mitochondrial Ca^{2+} and cytosolic ATP levels cells were plated onto 4-well Lab-Tek chamber slides and transfected using Effectene (Qiagen) 24 h prior the experiments either with the plasmid coding for mitochondrially targeted ratiometric GEM-GECO-1 (Addgene plasmid 32461), or with the plasmid coding for Cyt GO-ATeam 1 (kindly provided by Dr. H. Imamura, Kyoto University, Japan), respectively, and processed as previously described (Zhao et al., 2011; Nakano et al., 2011). Experiments were performed in 2.5 mM glucose HCSS with either 2 mM $CaCl_2$ or 100 μm EGTA. Additions were made as a bolus or by changes in the medium composition during continuous superfusion. Cells were excited for 100 ms at 436/20 nm for Mit-GEM-GECO1 and at 485/27 nm for GO-ATeam 1, and the emitted fluorescence was collected through a dual pass dichroic CFP-YFP (440–500 and 510–600 nm) alternatively at 480/40 nm (CFP) and 535/30 nm (YFP) for Mit-GEM-GECO-1, and through a FF495-Di03 dichroic at 520/35 nm (GFP) and 567/15 nm (OFP) for GO-ATeam probe. Images were collected every 5 s using a filter wheel (Lambda 10-2, Sutter Instruments; all filters purchased from Chroma) and recorded by a Hamamatsu C9100-02 camera mounted on an Axiovert 200M inverted microscope equipped with a 40×/1.3 Plan-Neofluar

Table 1. Glucose utilization in WT and *aralar* KO cultured neurons

Genotype	Glucose consumed (μmol/mg/h)	Lactate net form (μmol/mg/h)	%Lac/Gluc	Pyr consumed (μmol/mg/h)
WT	0.87 ± 0.211	1.09 ± 0.22	1.25	1.26 ± 0.07
aralar KO	0.64 ± 0.17	1.03 ± 0.31	1.54	1.74 ± 0.08***

Cortical neurons were cultured for 9–10 DIV (days *in vitro*) and subsequently incubated for 24 h in free-serum B27-supplemented neurobasal-A medium with 10 mM glucose. Experiments were performed at a final glucose concentration of 5 mM, 240 μM lactate, and 367 μM pyruvate. Results are mean ± SEM (n = 7–15) of two to four independent experiments. Data were statistically evaluated by one-way ANOVA followed by Student's t test. Comparisons between control and ARALAR-deficient cultures were significant where indicated; ***$p \leq 0.001$.

objective. Mit-GEM-GECO1 emission ratio was CFP/YFP, whereas GO-ATeam emission ratio was OFP/GFP reflecting mitochondrial Ca^{2+} and cyt ATP levels, respectively. For Mit-GEM GECO1 imaging ROIs were selected on mitochondrial-containing areas (identified based on their morphology). Single-cell fluorescence recordings were analyzed using ImageJ (NIH) or MetaMorph (Universal Imaging). When required, 50 μM BAPTA-AM (Sigma-Aldrich) loading was performed in Ca^{2+}-free HCSS during 30 min, and then washed and equilibrated in HCSS 2 mM $CaCl_2$ for another 30 min.

Measurement of cellular oxygen consumption. Cellular oxygen consumption rate (OCR) was measured using a Seahorse XF24 Extracellular Flux Analyzer (Seahorse Bioscience; Qian and Van Houten, 2010). Cortical primary neuronal were plated in XF24 V7 cell culture at 1.0×10^5 cells/well and incubated for 10 d in a 37°C, 5% CO_2 incubator in serum-free B27-supplemented neurobasal medium with high levels of glucose. To study OCR at lower glucose concentrations, cultures were preconditioned for 24 h in serum-free B27-supplemented neurobasal-A media with 10 mM glucose, with medium changes every 12 h. Cells were equilibrated with bicarbonate-free low-buffered DMEM medium (without pyruvate, lactate, glucose, glutamine, and Ca^{2+}) supplemented with 15, 5, or 2.5 mM glucose and 2 mM $CaCl_2$ or 100 μM EGTA in conditions of $\pm Ca^{2+}$, for 1 h immediately before extracellular flux assay. In experiments with isosmotic high K^+, cultures were first preconditioned for 20 min in 5 mM glucose HCSS in the presence or absence of 2 mM $CaCl_2$. Then, neurons were either maintained in the same medium or stimulated with 30 mM KCl in 5 mM glucose in Ca^{2+}-containing or Ca^{2+}-free isosmotic HCSS medium in which 30 mM NaCl was replaced by 30 mM KCl for 25 min before starting respirometry experiments. Calibration of the respiration took place after the vehicle injection in port A. BAPTA-AM was used at 50 μM in experiments with veratridine and carbachol in DMEM medium or 10 μM BAPTA-AM in the case of isosmotic KCl stimulation in HCSS medium. Loading was performed in Ca^{2+}-free in bicarbonate-free media or HCSS media for 20–30 min, and then washed and equilibrated in 2 mM $CaCl_2$ medium for another 25–30 min. Substrates were prepared in the same medium in which the experiment was conducted and were injected from the reagent ports automatically to the wells at the times indicated. Mitochondrial function in neurons was determined through sequential addition of 6 μM oligomycin, 0.5 mM 2,4-dinitrophenol, and 1 μM antimycin/1 μM rotenone. This allowed determination of basal oxygen consumption, oxygen consumption linked to ATP synthesis (ATP), non-ATP linked oxygen consumption (leak), mitochondrial uncoupled respiration (MUR), and nonmitochondrial oxygen consumption (NM; Qian and Van Houten, 2010; for review, see Brand and Nicholls, 2011).

Results

Glucose utilization in WT and *aralar* KO and *SCaMC-3* KO cultured neurons

Glucose consumption and net lactate formation were measured in culture media from neuronal cultures at 9 DIV using 5 mM glucose over 30–120 min incubation period (Table 1). ARALAR deficiency decreased glucose consumption (by 1.35-fold, $p = 0.4$, Student's t test, n = 7–15) but did not change lactate formation, unlike previous results obtained using higher glucose concentrations (Pardo et al., 2011). As a result, the percentage of glucose converted into lactate (%Lac/Gluc) tended to increase in *aralar* KO neurons. In addition, pyruvate consumption was significantly increased, by 1.39-fold ($p = 0.00047$, Student's t test), in *aralar* KO neurons (Table 1). These results show that neurons depend on ARALAR for malate/aspartate shuttle activity and glucose oxidation as previously described (Pardo et al., 2011). Glucose utilization and lactate production were the same in *SCaMC-3*-WT and *SCaMC-3*-KO neurons (1.10 ± 0.11 and 1.20 ± 0.13 micromoles glucose × mg prot^{-1} × h^{-1}, and 1.6 ± 0.2 and 2.2 ± 0.4 μmoles lactate × milligrams prot^{-1} × h^{-1} in *SCaMC-3*-WT and *SCaMC-3*-KO, respectively).

Bioenergetic characterization of control and *aralar* KO and *SCaMC-3*-KO cultured neurons

We next analyzed the respiratory activity in intact primary neuronal cultures by using a Seahorse XF24 extracellular flux analyzer (Qian and Van Houten, 2010). The basic setup of these experiments and the information obtained is shown in a graphic form in Figure 1*A*. In control experiments 2,4-dinitrophenol was titrated to obtain the maximum activity of the electron transport chain (data not shown). In other set of controls oligomycin was omitted to correct for its possible effects on the estimation of the maximal uncoupled coupled respiration (Brand and Nicholls, 2011). Under the assay conditions used, no effects of oligomycin on maximal uncoupled respiration were observed (data not shown).

The influence of Ca^{2+} on respiration was addressed by conducting the experiments in the presence and absence of 2 mM $CaCl_2$ in the incubation medium (Fig. 1*B*,*E*). The relative roles of ARALAR-MAS and SCaMC-3 in the stimulation of OCR were studied by using primary neuronal cultures derived from *aralar* (Fig. 1*A*–*E*) or *SCaMC-3*-KO mice (Fig. 1*C*,*D*,*F*). To control for the variations among the parental mouse strains, the wild-type condition in experiments with ARALAR- or SCaMC-3-deficient neurons was that of the specific parental strain (*aralar* WT or *SCaMC-3*-WT, respectively). Figure 1*G*,*H* illustrates the profiles obtained from WT and *aralar* KO cultures with 2.5 mM glucose in the presence or absence of Ca^{2+} and in the presence or absence of 2 mM pyruvate. The behavior of *SCaMC-3*-KO neuronal cultures was similar to that of WT neurons (Fig. 1*D*).

MUR

MUR in cultured neurons reflects the maximal respiratory capacity of neuronal mitochondria in intact neurons. It is not affected by the control exerted by proton reentry either through ATP synthase or the proton leak. It is mainly controlled by substrate supply, by the intrinsic respiratory capacity of mitochondria, and by nonmitochondrial respiration (Brand and Nicholls, 2011). Nonmitochondrial respiration was subtracted to calculate MUR and other mitochondrial respiratory parameters.

MUR was found to increase with the glucose concentration (Fig. 1*B*,*C*) and was higher in the presence than absence of Ca^{2+}. The lack of ARALAR caused a drastic decrease in MUR, both in Ca^{2+}-free and Ca^{2+}-containing media, at all glucose concentrations, dropping to 20% of WT values at 2.5 mM glucose (Fig. 1*B*; in the presence of Ca^{2+} MUR was 667.94 ± 114.36 in WT vs 154.63 ± 31.39 in *aralar* KO neurons, Student's t test, $p = 0.009$), which is consistent with the limitation in glucose-derived pyruvate supply to mitochondria when the major NADH shuttle system fails. Indeed, exogenous pyruvate (but not lactate, results not shown) supply, which bypasses the limitation imposed by the lack of MAS, did not change MUR in the presence of Ca^{2+} (a nonsignificant 1.23-fold increase; Fig. 1*G*,*I*) but increased it significantly, by ~2.17-fold both in the presence and 1.93-fold in

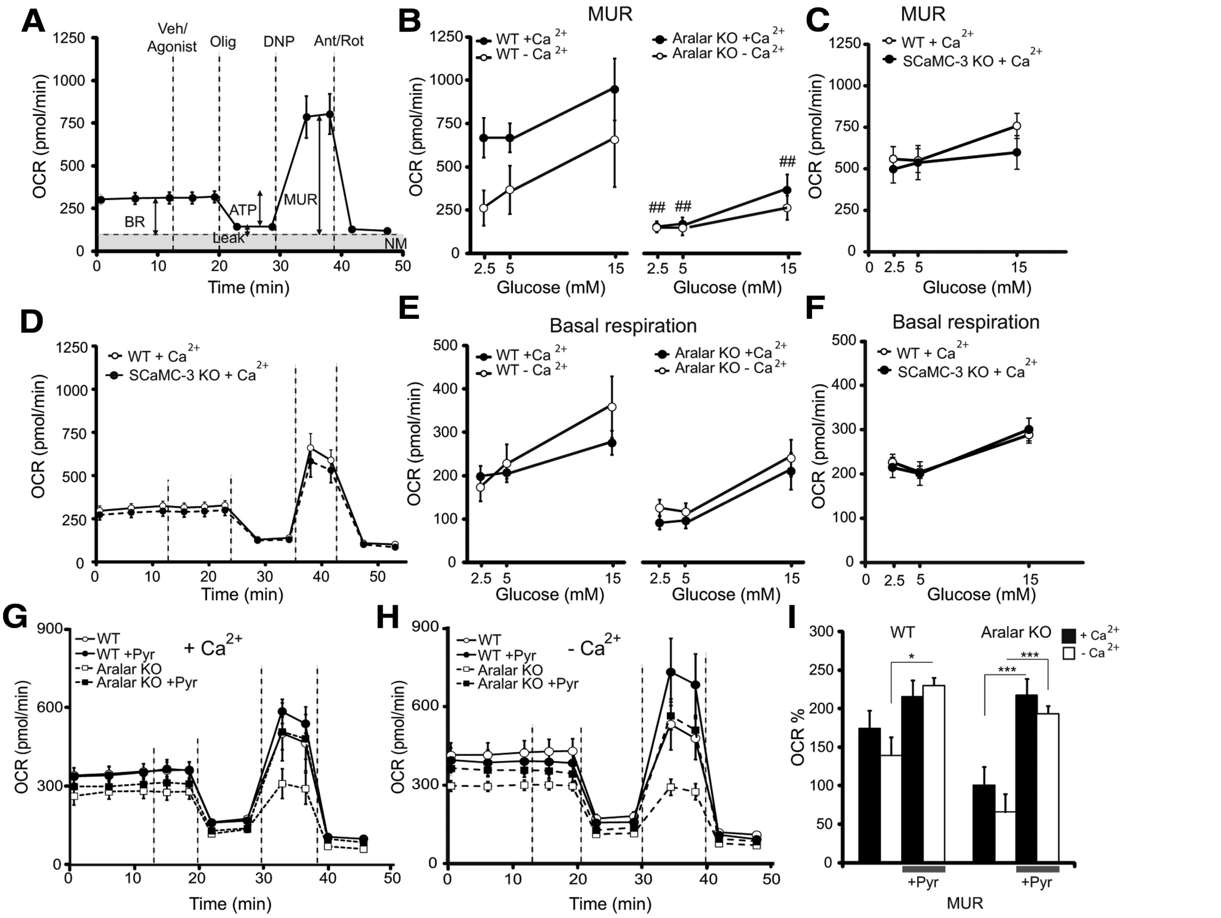

Figure 1. Bioenergetic characterization of *aralar* WT, *aralar* KO, *SCaMC-3*-WT, and *SCaMC-3*-KO cultured neurons. ***A***, Representative pharmacological profile of oxygen consumption rate in *aralar* WT neurons showing the sequential injection of agonist/vehicle (Veh) and metabolic inhibitors: oligomycin (Olig, 6 μM), 2,4-dinitrophenol (DNP, 0.5 mM) and antimycin A/rotenone (Ant/Rot, 1.0 μM/1.0 μM) at different time point indicated by dashed lines which allows the determination of basal oxygen consumption (BR), oxygen consumption linked to ATP synthesis (ATP), non-ATP linked oxygen consumption (Leak), maximal uncoupled respiration (MUR) and nonmitochondrial oxygen consumption (NM) as represented graphically. ***B***, ***C***, Effect of glucose and Ca^{2+} on maximal uncoupled respiration (MUR) in *aralar* WT vs *aralar* KO neurons and *SCaMC-3*-WT versus *SCaMC-3*-KO neurons. ***D***, Oxygen consumption rate in *SCaMC-3*-WT versus KO neurons in 2.5 mM glucose, 2 mM Ca^{2+}. ***E***, ***F***, Effect of glucose and Ca^{2+} on basal respiration capacity in *aralar* WT versus *aralar* KO and *SCaMC-3*-WT versus *SCaMC-3*-KO neurons. Results are means ± SEM of 3–11 experiments. The effect of Ca^{2+} on MUR was significant for *aralar* WT ($p < 0.05$, two-way ANOVA) but not *aralar* KO neurons, and the lack of ARALAR caused a significant decrease in MUR at all glucose concentrations in the absence ($p < 0.05$, two-way ANOVA) or presence of Ca^{2+} ($p < 0.001$, two-way ANOVA; ##$p < 0.01$, *post hoc* Bonferroni test). Glucose, but not Ca^{2+}, had a significant effect on basal respiration both in *aralar* WT ($p < 0.01$, two-way ANOVA) and *aralar* KO neurons ($p < 0.001$, two-way ANOVA) and the lack of ARALAR caused a significant decrease in basal respiration both in the presence ($p < 0.001$, two-way ANOVA) or absence ($p < 0.01$, two-way ANOVA) of Ca^{2+}. ***G***, ***H***, Oxygen consumption profile in *aralar* WT and *aralar* KO cultures in 2.5 mM glucose medium supplemented with 2 mM pyruvate (Pyr) in the presence and absence of 2 mM Ca^{2+}. ***I***, MUR in the presence or absence of 2 mM pyruvate, expressed as percentage of basal OCR in *aralar* WT and *aralar* KO neurons ($n = 3$–11 experiments, Student's *t* test; *$p \leq 0.05$, ***$p \leq 0.001$). Data are expressed as mean ± SEM. Statistical analysis was performed using STATISTICA, version7, StatSoft.

the absence of Ca^{2+} ($p = 0.0009$ and $p = 0.00013$ respectively, Student's *t* test) in *aralar* KO neurons (Fig. 1*G–I*). We did not find any effect of 10 mM lactate on MUR in WT or *aralar* KO neurons (results not shown). This may be due to the strong cytosolic acidification induced by the uptake of lactic acid (Álvarez et al., 2003) which may inhibit glycolysis. Therefore, the effect of lactate has not been studied any further.

As indicated above (Fig. 1*B*), MUR tended to be higher in the presence than in the absence of external Ca^{2+} at every glucose concentration. This could reflect an effect of cytosolic Ca^{2+} on substrate supply, perhaps by activating the malate aspartate shuttle. Indeed, the effect of Ca^{2+} on MUR was no longer present in ARALAR-deficient neurons especially at the physiological glucose concentrations of 2.5 and 5 mM. On the other hand pyruvate increases MUR in *aralar* KO neurons regardless of the presence of Ca^{2+} while in control neurons this effect is less prominent and only in Ca^{2+}-free media (Fig. 1*G–I*). Indeed, as the presence of the uncoupler prevents Ca^{2+} uptake in mitochondria and Ca^{2+}-activation of pyruvate dehydrogenase, it is expected to result in a Ca^{2+}-independent respiration on pyruvate. These results are consistent with recent reports showing that removal of the components of the mitochondrial Ca^{2+} uniporter complex (MCU, MICU1, MCUR1) does not change MUR (Baughman et al., 2011; Mallilankaraman et al., 2012a,b) whereas preventing IP3-mediated Ca^{2+} signals does reduce MUR (Cárdenas et al., 2010).

Basal respiration

Basal respiration rates increased with glucose concentration in WT, *aralar* KO, and *SCaMC-3*-KO neurons, and this was independent of the presence of Ca^{2+} (Fig. 1*E*). This is unexpected because the Km for hexokinase is very low, 0.05 mM (Grossbard and Schimke, 1966), but could be related to mild osmotic changes with higher glucose level. The presence or absence of 2 mM pyruvate did not change basal respiration in 2.5 mM glucose in WT, *aralar* KO, or *SCaMC-3*-KO neurons (Fig. 1*G*,*H*, and results not shown).

Remarkably with 2.5 mM glucose, a concentration close to that normally present in cerebral extracellular fluid *in vivo* (Lewis et al., 1974), absolute OCR in *aralar* KO neuronal cultures, was reduced by 46.13 ± 7.46% ($p = 0.0067$, Student's *t* test) with respect to WT or *SCaMC-3*-KO neuronal cultures (Fig. 1*E*,*F*). The decrease in OCR in *aralar* KO neurons persisted at all glucose concentrations indicating that the lack of MAS prevents adequate glucose-derived substrate supply to mitochondria also under basal conditions. However, the fact that basal respiration still proceeds even if halved, suggests the existence of other shuttle systems in these neurons. The participation of mitochondrial ATP synthesis in basal respiration is estimated from the decrease in respiration after the addition of oligomycin. Respiration in the presence of oligomycin reflects the proton leak but as ATP synthase inhibition results in a slight mitochondrial hyperpolarization and the proton leak is voltage-dependent, this approach underestimates ATP synthesis and exaggerates the real proton leak (Brand and Nicholls, 2011). With these caveats, the percentage of OCR involved in ATP synthesis in WT and *aralar* KO neurons in 2.5 mM glucose was the same, 73.92 ± 1.20%, and the corresponding proton leak is 26.08 ± 1.20%, with an "apparent" mitochondrial respiratory control ratio (ATP synthesis/proton leak) of 3.63 ± 0.56. The presence of pyruvate or the absence of SCaMC-3 (results not shown) did not change the apparent respiratory control ratios (RCR) under basal conditions, but it should be noted that both *SCaMC-3*-WT and *SCaMC-3*-KO neurons had higher apparent RCR values with respect to *aralar* WT or *aralar* KO neurons, of 5.1 ± 0.48 (*SCaMC-3*-WT) and 6 ± 0.3 (*SCaMC-3*-KO) in 2 mM Ca^{2+} medium, and of 6.08 ± 0.28 (*SCaMC-3*-WT) and 5.85 ± 1.01 (*SCaMC-3*-KO) in Ca^{2+}-free medium, these differences should be consequence of the different parental mouse strains.

Effect of agonists on regulation of OCR

Having shown that in neurons using 2.5–5 mM glucose, basal respiration is not limited by substrate supply, we next studied the control of respiration by agents able to increase neuronal workload. Any increase in workload is followed by ATP breakdown and ADP production which is expected to increase OCR. We used veratridine and high K^+ which increase workload after plasma membrane depolarization through increases in cytosolic Na^+ and Ca^{2+} and stimulation of the Na^+-K^+ ATPase, Na^+/Ca^{2+} exchange and the sarcoendoplasmic reticulum Ca^{2+}-ATPase (SERCA) and plasma membrane Ca^{2+}-ATPase (PMCA) pumps. It is expected that in the presence, but not absence, of external Ca^{2+}, Ca^{2+}-regulation of respiration would contribute to the increase in OCR in response to these workloads. It has been proposed that even Ca^{2+} alone, not ATP demand, stimulates mitochondrial bioenergetics in some neuronal types (Chouhan et al., 2012).

Another way to increase workload is through agents causing Ca^{2+}-mobilization from intracellular stores. The increase in cytosolic Ca^{2+} will cause ATP breakdown by SERCA and PMCA pumps and would be expected to increase OCR. ATP utilization to recover the resting state is much smaller than that caused by Na^+ entry (Attwell and Laughlin, 2001) and consequently, the OCR response should be also smaller. Moreover, removal of external Ca^{2+} in this condition will reduce Ca^{2+} signals and workload at the same time.

In either workload condition, Ca^{2+} may activate OCR by activating ARALAR-MAS and/or SCaMC-3, by way of increasing substrate or adenine nucleotide supply to mitochondria, and Ca^{2+} may enter mitochondria through the recently identified MCU (Baughman et al., 2011; De Stefani et al., 2011), increasing NADH production in mitochondria and oxidative phosphorylation (Glancy and Balaban, 2012). These mechanisms differ in their $S_{0.5}$ values for Ca^{2+}-activation, ~300 nM for ARALAR/AGC1 (Pardo et al., 2006) and in the micromolar range for both SCaMC-3 (Amigo et al., 2013) and MCU (Drago et al., 2011). The relative roles of these pathways in the stimulation of OCR were studied by using primary neuronal cultures derived from *aralar* or *SCaMC-3*-KO mice. To control for the variations among the parental mouse strains, the wild-type condition in experiments with ARALAR- or SCaMC-3-deficient neurons was that of the specific parental strain (*aralar* WT or *SCaMC-3*-WT, respectively).

Veratridine-induced increase in respiration is activated by Ca^{2+} and results in a drop in ATP levels

The lipophilic alkaloid neurotoxin, veratridine, binds buried sites in the voltage-dependent Na^+ channels in the matrix of the lipid bilayer (Strichartz et al., 1987), causing Na^+ channels to remain open, and a pronounced increase in intracellular Na^+ concentration (Rose and Ransom, 1997). The plasma membrane depolarization produced by veratridine opens voltage-dependent Ca^{2+} channels allowing Ca^{2+} inflow (Rego et al., 2001). Figure 2 shows the effects of veratridine in cortical neurons. Veratridine (50 μM) produced a large and sustained increase in $[Ca^{2+}]_i$ which was prevented in Ca^{2+}-free media (Fig. 2*A*,*B*). It also induced a sustained rise in mitochondrial Ca^{2+} levels, reported by mit-GEM-GECO-1, a genetically coded Ca^{2+} sensor expressed in the mitochondrial matrix (Zhao et al., 2011) which was completely absent in Ca^{2+}-free media (Fig. 2*D*,*E*). Cytosolic ATP levels, measured with the low affinity FRET cytosolic ATP sensor GO-ATeam1 (Nakano et al., 2011), were found to drop after veratridine exposure, particularly in Ca^{2+}-free media (Fig. 2*G*–*I*). Veratridine induced a sharp increase in OCR of mouse cortical neurons, as previously observed in synaptosomes (Brand and Nicholls, 2011) which resulted in 180.21 ± 4.76% (*aralar* WT) to 255.02 ± 11.01% (*SCaMC-3*-WT) increase over basal levels (Figs. 2*J*, 3*E*–*G* and *A*–*C*, respectively). The increase was due to coupled respiration and proton leak, as apparent respiratory control values (Figs. 2*L*, 3*D*,*H*) did not change significantly after veratridine addition in Ca^{2+} media.

In the absence of Ca^{2+}, the increase in OCR induced by veratridine was greatly reduced (Figs. 2*J*, 3*B*, *F*). Proton leak values after veratridine exposure were higher in the presence than in the absence of Ca^{2+} in the external medium, as reflected in the higher RCR in Ca^{2+}-free than Ca^{2+}-containing medium (Figs. 2*L*, 3*D*, *H*). This is likely due to the existence of Ca^{2+} cycling across the inner mitochondrial membrane through MCU, H^+/Ca^{2+}, Na^+/Ca^{2+}, and H^+/Na^+ exchangers (Nicholls, 2005).

The veratridine-induced increase in OCR in Ca^{2+}-free media is driven by the increase in cytosolic Na^+ coupled to ATP demand. In the presence of Ca^{2+}, the increase in OCR induced by veratridine is even higher, whereas ATP levels dropped significantly less (Fig. 2*I*). This may be caused by (1) the increases in cytosolic Na^+ and Ca^{2+} which could result in a further increase in ATP demand in the presence of Ca^{2+}, or (2) the absence of Ca^{2+}-dependent regulation of respiration in Ca^{2+}-free media. To tell apart these possibilities, neurons were preincubated with the rapid intracellular Ca^{2+}-chelator BAPTA-AM (Abramov and Duchen, 2008) and challenged with veratridine in the presence of Ca^{2+}. BAPTA loading blunts cytosolic Ca^{2+} signals but does not change Ca^{2+} inflow through voltage-dependent Ca^{2+} channels (Adler et al., 1991), conditions under which the Ca^{2+}-dependent fraction of the global workload induced by veratridine is maintained. In BAPTA-AM (50 μM) loaded neurons Ca^{2+} signals in the cytosol, and specially in mitochondria, only appeared gradually and after a substantial delay (Fig. 2*A*,*C*) and veratridine-stimulation of OCR was severely decreased (Fig. 2*J*), indicating that Ca^{2+}-signaling is clearly required for veratridine-induced stimulation of respiration in Ca^{2+}-medium.

We also tested whether the Na^+-dependent fraction of workload induced by veratridine was maintained in the absence or presence of Ca^{2+}. Intracellular Na^+ was measured in neurons loaded with SBFI-AM, the Na^+ indicator (Rose and Ransom, 1997; Fig. 2*M*–*O*). As initial SBFI ratios are slightly higher in Ca^{2+}-free than in Ca^{2+}-containing medium, they were normalized to the initial SBFI ratio. Figure 2*O* clearly shows that the absence of Ca^{2+} did not modify veratridine-induced Na^+ influx. As veratridine-induced drop in cytosolic ATP was still more pronounced in Ca^{2+}-free media, together the results suggest that the lack of Ca^{2+}-regulation of OCR prevents an adequate regeneration of ATP to meet.

Veratridine- and Ca^{2+}-dependent stimulation of respiration is blunted in the absence of SCaMC-3 and ARALAR

The stimulatory effect of veratridine was different in WT and *SCaMC-3*-KO neu-

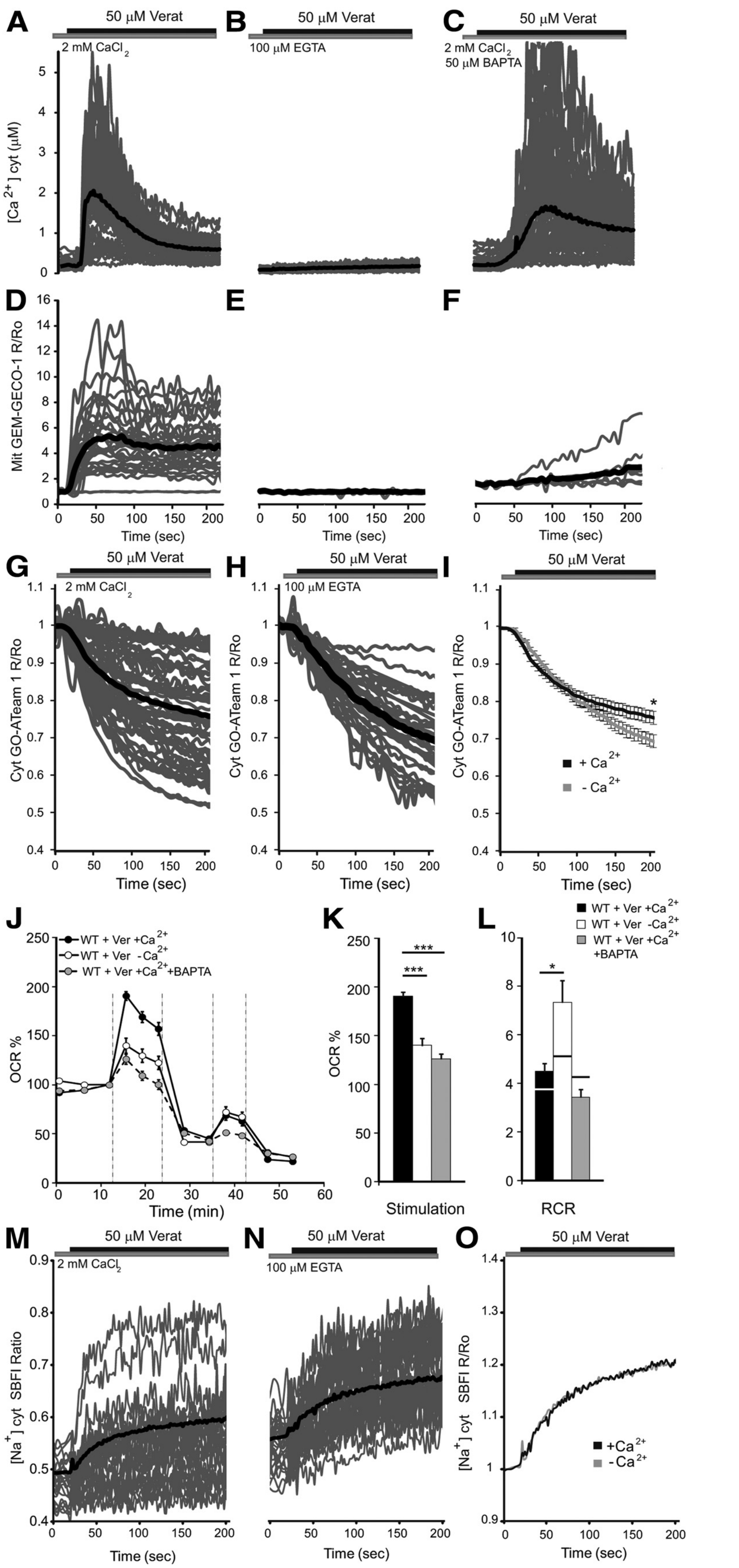

Figure 2. Changes in cytosolic and mitochondrial Ca^{2+}, cytosolic ATP, oxygen consumption and cytosolic Na^+ in primary neuronal cultures in response to veratridine. ***A–C***, Changes in $[Ca^{2+}]_{cyt}$, in Fura-2 loaded neurons obtained by stimulation with 50 μM Veratridine (Ver or Verat) in 2 mM Ca^{2+}, Ca^{2+}-free medium, or 50 μM BAPTA preloaded neurons in 2 mM Ca^{2+} medium. ***D–F***, Corresponding data in neurons transfected with Mit-GEM-GECO1 probe to determine changes in $[Ca^{2+}]_{mit}$. Recordings from at least 60 cells per condition and two independent experiments were used for $[Ca^{2+}]_i$ and a minimum of 15 cells and eight independent experiments for $[Ca^{2+}]_{mit}$ imaging. Individual cell recordings (gray) and average (thick black trace) were shown. ***G–I***, Cytosolic ATP in neurons transfected with cyt-GO-ATeam1 stimulated with veratridine in 2 mM Ca^{2+} medium, Ca^{2+}-free medium plus 100 μM EGTA and comparison of the two conditions. Recordings from individual cells (gray) and average (black) are shown. The drop of ATP values with respect to basal levels 200 s after veratridine addition were 23.9 ± 1.70% in the presence and 30 ± 1.69% in the absence of Ca^{2+} (* $p = 0.017$ two-tailed unpaired Student's *t* test). ***J***, Veratridine-induced stimulation of OCR in *aralar* WT neurons under the mentioned Ca^{2+} and BAPTA conditions. ***K***, ***L***, Stimulation of respiration (as percentage of basal values) and RCR. RCR in nonstimulated state are represented with horizontal lines for each experimental condition ($n = 9–11$ experiments one-way ANOVA, * $p \leq 0.05$, *** $p \leq 0.001$, *post hoc* Bonferroni test). ***M***, ***N***, Changes in $[Na^+]_i$, in SBFI-loaded neurons by stimulation with 50 μM veratridine in 2 mM Ca^{2+} medium or Ca^{2+}-free medium (∼90 neurons per condition). ***O***, Comparison between response in Ca^{2+} medium (black trace) and Ca^{2+}-free (gray trace) is shown. Increases in normalized SBFI ratio 200 s after veratridine were 21.1 ± 1.02% and 20.3 ± 0.81in the presence or absence of Ca^{2+}, respectively.

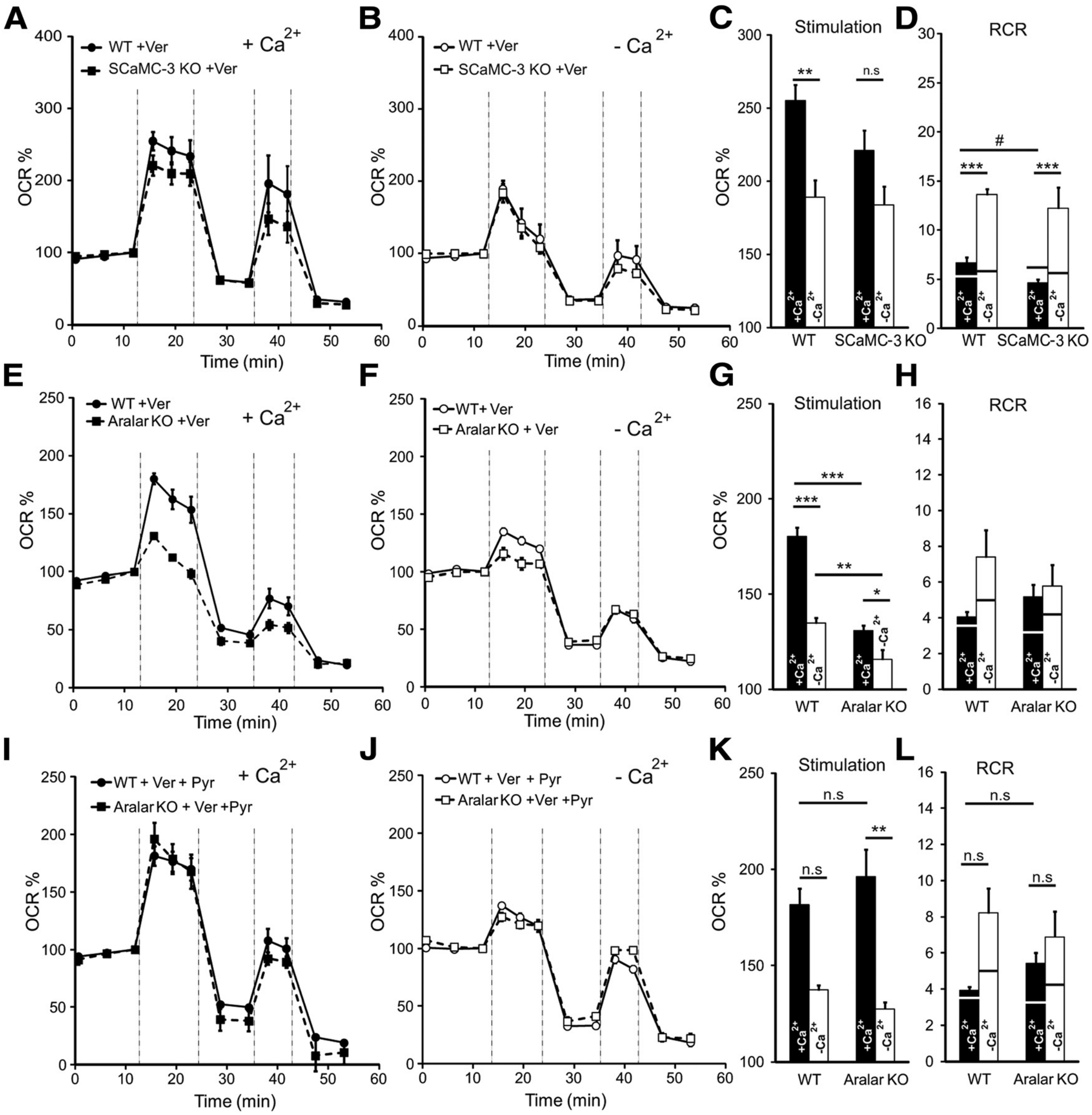

Figure 3. OCR responses to veratridine in ARALAR- and SCaMC-3-deficient neurons. ***A–D***, Respiratory profiles in the presence or absence of 2 mM Ca^{2+}, stimulation of mitochondrial respiration and RCRs of *SCaMC-3*-WT and *SCaMC-3*-KO neurons stimulated with 50 μM Veratridne (Ver) in 2.5 mM glucose. ***E–H***, Corresponding data from *aralar* WT and *aralar* KO neurons. ***I–L***, Corresponding data for the effect of 2 mM pyruvate (Pyr) on veratridine-induced mitochondrial respiration in *aralar* WT and *aralar* KO neurons. RCR in nonstimulated state are represented with horizontal lines for each experimental condition. Data are expressed as mean ± SEM from $n = 5–6$ experiments in *SCaMC-3*-WT and *SCaMC-3*-KO cultures, and from $n = 4–12$ experiments in *aralar* WT and *aralar* KO cultures. Two-way ANOVA, $^{*}p \leq 0.05$; $^{**}p \leq 0.01$; $^{***}p \leq 0.001$, *post hoc* Bonferroni test.

rons (Fig. 3*A–D*). In the presence of Ca^{2+}, the increase in OCR was significantly smaller in *SCaMC-3*-KO neurons than in controls, but these differences disappeared in Ca^{2+}-free media (Fig. 3*C*). The requirement for Ca^{2+} in the effect of SCaMC-3 points to a potential effect of Ca^{2+}-activation of the transporter in the acquisition of a full increase in respiration. This is related with an increase in coupled respiration, as proton leak values are unchanged in *SCaMC-3*-KO neurons, resulting in significantly higher RCR values in WT than in *SCaMC-3*-KO neurons (Fig. 3*D*).

The stimulatory effect of veratridine was strikingly diminished in *aralar* KO neurons both in the presence and in the absence of Ca^{2+} (Fig. 3*E–H*). It should be noted that as the basal rates in the *aralar* KO cells are about half those of the WT (with or without calcium), the decrease in %OCR stimulation caused by veratridine shown in Figure 3*E*,*F*, actually represents a very large difference in absolute OCR. *aralar* KO neurons respond to veratridine in a Ca^{2+}-dependent way (Fig. 3*G*), thus Ca^{2+} entry in mitochondria and activation of dehydrogenases together with activation of SCaMC-3 provide the only pathways of Ca^{2+} regulation of mitochondrial respiration in these neurons.

To analyze whether the lower response to veratridine was due to limited substrate supply to mitochondria, the effect of pyruvate was analyzed in this experimental condition. We found that pyruvate (2 mM) did not increase veratridine-stimulated respiration in WT, but caused an impressive threefold increase in stimulated respiration in *aralar* KO neurons (Fig. 3, compare *G* and *K*) reaching stimulation values identical to those of WT neurons both in the absence or presence of Ca^{2+} (Fig. 3*I–L*). These results clearly show that the failure to respond to veratridine in *aralar* KO neurons is due to substrate limitation imposed by the lack of MAS.

High K^+ induced increase in mitochondrial respiration is highly Ca^{2+}-dependent

High extracellular KCl concentration (30 mM) depolarizes cell membrane, activating the voltage-sensitive Na^+ and Ca^{2+} channels leading to elevation of their cytosolic concentrations in cultured neurons (Courtney et al., 1990; Rose and Ransom, 1997). Channel opening is transient due to the voltage-dependent inactivation of Na^+ channels but some of the Ca^{2+} channels remain open under continuous depolarization (Courtney et al., 1990). The increase in cytosolic Na^+ and Ca^{2+} levels will activate Na^+ and Ca^{2+} extrusion mechanisms (Na^+/K^+ ATPase pump, SERCA, PMCA, and Na^+/Ca^{2+} exchangers), which will activate ATP turnover.

Figure 4*A–P* shows the responses to the addition of 30 mM KCl in cortical neurons. KCl addition produces a pronounced elevation of $[Ca^{2+}]_i$ in the presence, but not absence, of external Ca^{2+}, with average $[Ca^{2+}]_i$ returning to ~500 nM in the continuous presence of KCl (Fig. 4*A*,*B*). Mitochondrial Ca^{2+} levels increase in parallel to those of cytosolic Ca^{2+} levels, and this increase is absent in Ca^{2+}-free media (Fig. 4 *D*,*E*). The results were essentially the same when KCl addition was performed by isosmotic replacing Na^+ for K^+ during continuous superfusion (results not shown).

The changes in cytosolic ATP levels, after isosmotic replacement of 30 mM Na^+ for 30 mM K^+ are shown in Figure 4*G–I*. A gradual drop in cytosolic ATP levels is observed in the presence of Ca^{2+} but greater than that in the absence of Ca^{2+}. When 30 mM KCl was added as a bolus, this drop was preceded by a rapid transient increase which was the same in the absence or presence of Ca^{2+}, most likely caused by a hyperosmotic effect, as it is also observed after 30 mM NaCl or 60 mM sucrose addition (results not shown).

The experimental setup of the Seahorse equipment does not allow to add KCl in an isotonic medium. Therefore, we first evaluated the effect of 30 mM KCl addition on OCR in cortical neurons. High potassium produces an immediate increase in OCR of ~183% (*aralar* WT neurons; Fig. 4*J*,*K*) or 200% (*SCaMC-3*-WT neurons, data not shown) over basal values in the presence of 2 mM Ca^{2+} but a much smaller increase of ~117% (*aralar* WT; Fig. 4*J*,*K*) and 150% (*SCaMC-3*-WT, data not shown) respectively, in the absence of Ca^{2+}. This stimulation was stable >6–9 min and was not increased in the presence of pyruvate (results not shown). In PC12 cells, KCl effects on OCR are due to an hyperosmotic response (Ashton and Ushkaryov, 2005). However, in cortical neurons the effects of hyperosmotic NaCl or sucrose on OCR were much smaller than those of KCl (results not shown), suggesting that most of the OCR response to KCl addition is not due to the hyperosmotic effect.

We next evaluated the response to 30 mM KCl under isosmotic conditions. Neurons were incubated with isosmotic 30 mM KCl or control (5.4 mM KCl) conditions before OCR determinations were started. As observed, OCR was also increased in isosmotic 30 mM KCl, but slightly less than in hyperosmotic conditions. KCl stimulation was also calcium-dependent, 137.55 ± 8.09% and 113.97 ± 7.96% in the presence and absence of Ca^{2+}, respectively (Fig. 4*N*). Isosmotic KCl stimulation significantly increased oligomycin-sensitive respiration in the presence of 2 mM Ca^{2+} (77.24 ± 1.64 and 80.18 ± 0.65 in Ca^{2+}-containing basal and KCl stimulated conditions, respectively, $p = 0.025$, Student's *t* test).

To investigate the role of Ca^{2+}-regulation of OCR in the response to isosmotic KCl, neurons were preincubated with 10 μM BAPTA-AM, and challenged with KCl in the presence of Ca^{2+} to maintain the global workload of K^+-depolarization in a Ca^{2+}-medium, while blunting cytosolic Ca^{2+} signals. Indeed, Figure 4*C*,*F* shows that the increases in $[Ca^{2+}]_i$ and specially $[Ca^{2+}]_{mit}$ were drastically reduced and delayed under this condition. Interestingly, KCl-stimulation of OCR dropped to the values obtained in Ca^{2+}-free medium (Fig. 4*M*,*N*). By using neurons loaded with SBFI-AM we have found that isosmotic KCl causes only subtle changes in cytosolic Na^+ both in the presence or absence of Ca^{2+} (Fig. 4*P*), in agreement with previous reports (Rose and Ransom, 1997). This suggests that KCl-induced workload is probably related to the increase in cytosolic Ca^{2+}, whereas increased cytosolic Na^+ plays a modest role. This is consistent with the findings that (1) KCl-induced fall in cytosolic ATP is hardly detectable in Ca^{2+}-free medium (Fig. 4 *G–I*) and(2) KCl-stimulation of OCR was much lower in the absence than in the presence of Ca^{2+} (Fig. 4*N*). These results clearly indicate that Ca^{2+}-regulation of OCR is absolutely required to reach a full stimulation of coupled respiration by KCl-depolarization.

High K^+-stimulation of OCR requires ARALAR-MAS but not SCaMC-3

Figure 5*A–J* shows the effects of the lack of SCaMC-3 or ARALAR on K^+-stimulated OCR in cortical neurons under isosmotic conditions. The lack of SCaMC-3 did not modify the response to high K^+ (Fig. 5*A–C*). However, the lack of ARALAR blocked K^+-stimulation of OCR, both in the presence or absence of Ca^{2+}, suggesting that the Ca^{2+}-mediated stimulation strictly requires ARALAR-MAS. Indeed, although in WT neurons K^+-stimulated OCR was not increased any further in the presence of pyruvate (Fig. 5, compare *F* and *I*), the addition of 2 mM pyruvate, did not change basal OCR but led to a pronounced potentiation of the effects of K^+ on *aralar* KO neuron. In fact, stimulation values were now the same as in WT neurons. These results further indicate that the Ca^{2+}-dependent stimulation of OCR caused by KCl relies on ARALAR as signaling pathway to mitochondria.

Carbachol induces a Ca^{2+}-dependent increase in respiration levels which requires the ARALAR-MAS pathway

In cortical neurons, carbachol acts on muscarinic cholinergic, G-protein-coupled receptors, which activate $G_{q/11}$ and signal through activation of phospholipase C, generation of inositol 3-phosphate (IP_3) and Ca^{2+}-mobilization from intracellular stores, giving rise to a transient $[Ca^{2+}]_i$ peak (Kelly et al., 1996; Lucas-Meunier et al., 2003; Kipanyula et al., 2012). The emptying of the endoplasmic reticulum (ER) Ca^{2+} stores triggered by IP_3 activates Ca^{2+} entry through low-conductance plasmalemmal channels that are regulated by the level of Ca^{2+} stored in the ER, a process known as store-operated Ca^{2+} entry (SOCE; Putney, 2009).

Figure 6*A*,*B* shows that 250 μM carbachol induced an immediate increase in $[Ca^{2+}]_i$ also observed in Ca^{2+}-free medium, followed by a new steady-state $[Ca^{2+}]_i$ value above resting levels in the presence of Ca^{2+} or to a recovery of the resting state in Ca^{2+}-free media in which SOCE-induced Ca^{2+} entry does not occur. Carbachol-induced $[Ca^{2+}]_{cyt}$ signals hardly reached mitochondria, as no rise in $[Ca^{2+}]_{mit}$ was detected either in the presence or absence of Ca^{2+} (Fig. 6*D*,*E*). The workload induced by carbachol is much smaller than that involving plasma membrane depolarization and does not lead to any changes in cytosolic ATP levels either in the presence or absence of Ca^{2+} (Fig. 6*F*). As ATP is used to restore Ca^{2+} levels to resting conditions, ATP demand is expected to be drastically reduced in a Ca^{2+}-free medium. Accordingly, carbachol induced an increase in OCR in the presence of Ca^{2+} but not in its absence (Fig. 6*G–I*) but much

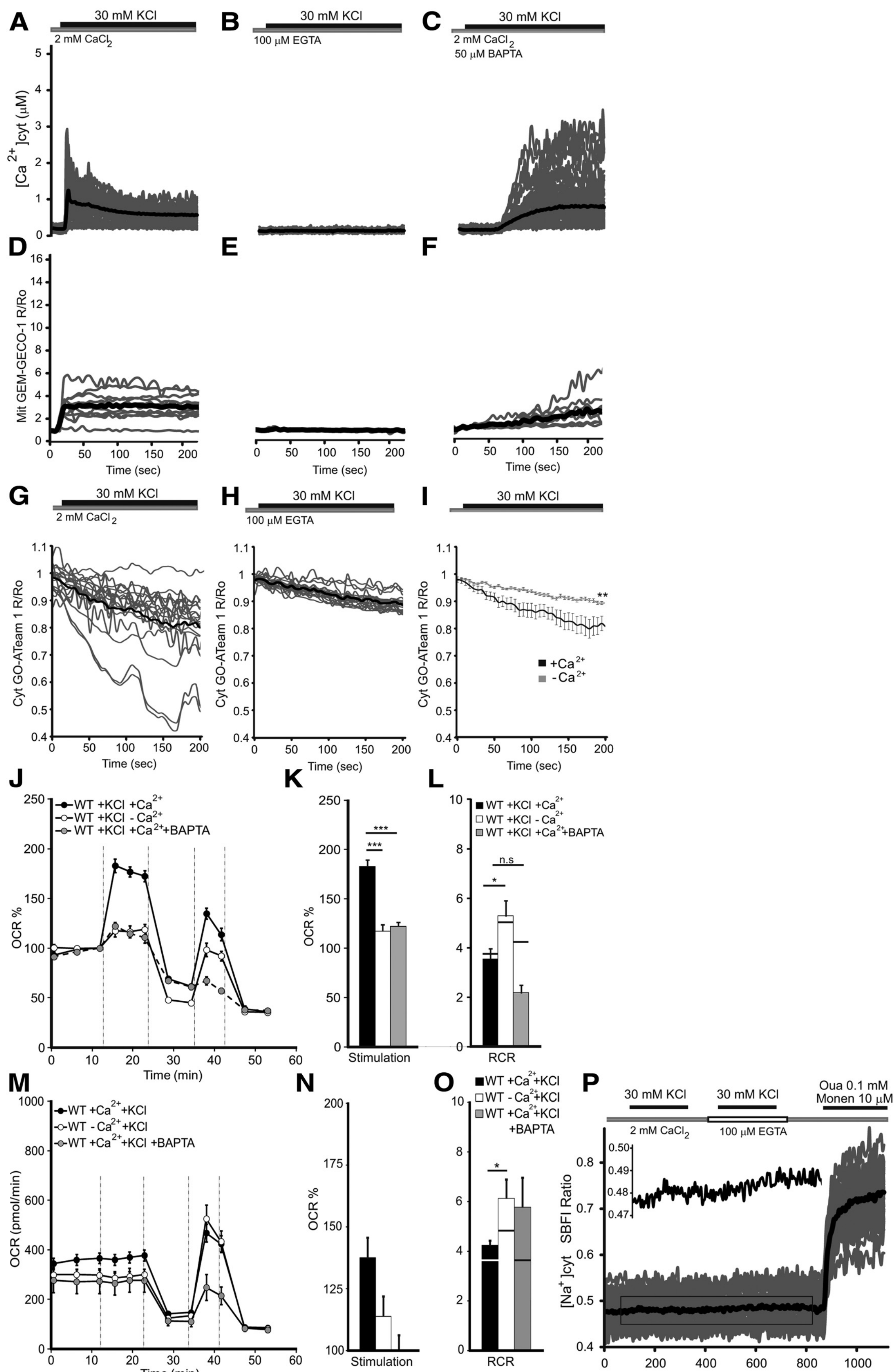

Figure 4. Changes of cytosolic and mitochondrial Ca^{2+}, cytosolic ATP, oxygen consumption, and cytosolic Na^{+} in primary neuronal in response to KCl. ***A–C***, Changes in $[Ca^{2+}]_{cyt}$, in Fura-2-loaded neurons obtained by stimulation with 30 mM KCl in 2 mM Ca^{2+}, Ca^{2+}-free medium, or 50 μM BAPTA preloaded neurons in 2 mM Ca^{2+} medium***.*** ***D–F***, (*Figure legend continues.*)

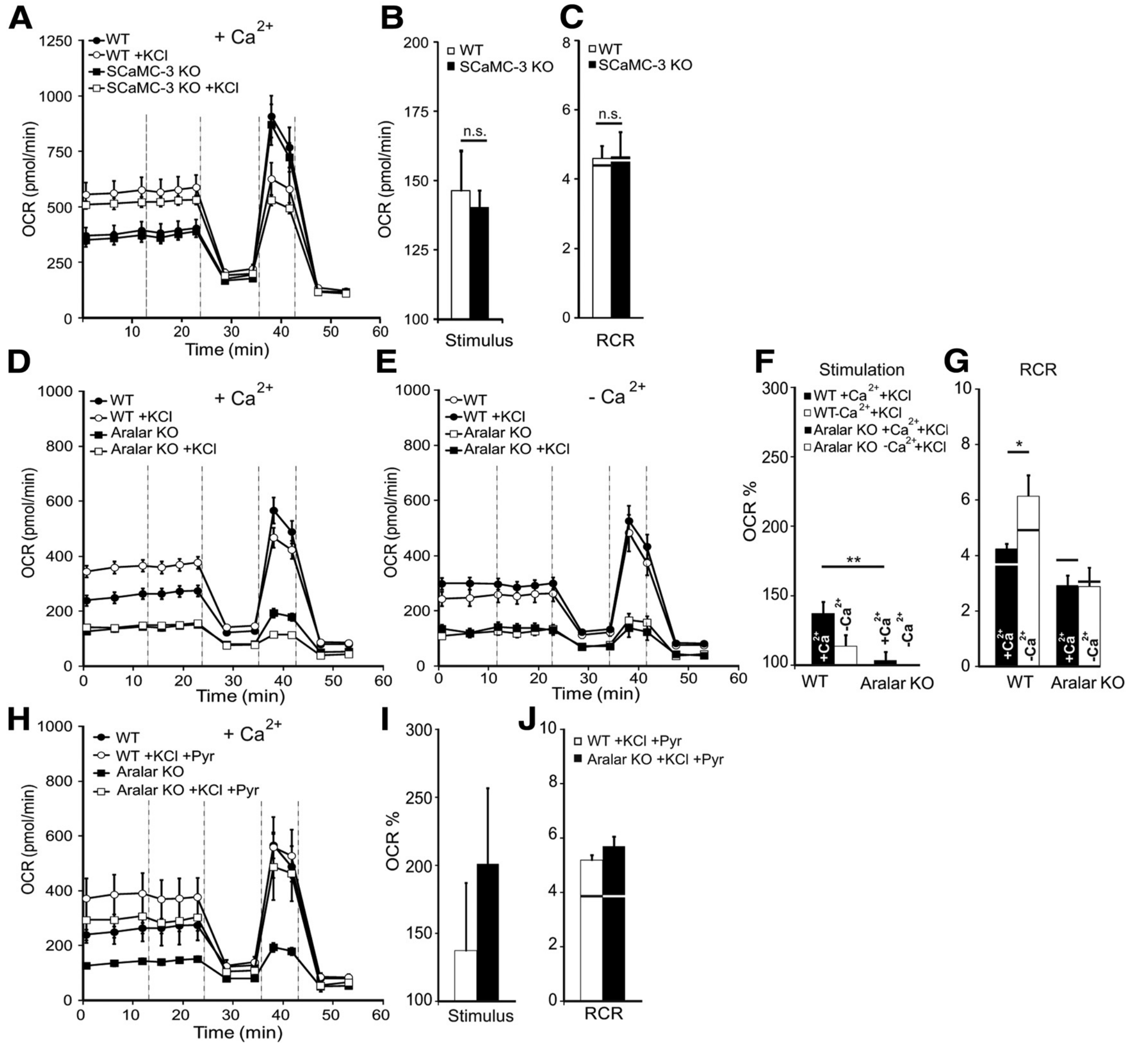

Figure 5. OCR-responses to 30 mM KCl in ARALAR- or SCaMC-3-deficient cortical neurons. ***A–C***, Respiratory profiles, stimulation of mitochondrial respiration, and RCRs of *SCaMC-3*-WT and *SCaMC-3*-KO neurons stimulated with isosmotic 30 mM KCl in the presence of 2 mM Ca^{2+}. ***D–G***, Corresponding data for *aralar* WT and *aralar* KO cultures in the presence or absence of 2 mM Ca^{2+}. ***H–J***, Corresponding data for the effect of 2 mM pyruvate (Pyr) on isosmotic 30 mM KCl-induced respiratory stimulation in *aralar* WT and *aralar* KO neurons in the presence of 2 mM Ca^{2+}. RCR in nonstimulated state are represented with horizontal lines for each experimental condition. Data correspond to 5–6 experiments in *SCaMC-3*-WT and *SCaMC-3*-KO cultures and 4–24 experiments in *aralar* WT and *aralar* KO respectively (two-way ANOVA, $^{*}p \leq 0.05$; $^{**}p \leq 0.01$; *post hoc* Bonferroni test).

←

(*Figure legend continued.*) Corresponding data in neurons transfected with Mit-GEM-GECO1 probe to determine changes in $[Ca^{2+}]_{mit}$. Recordings from at least 60 cells per condition and two independent experiments were used for cytosolic Ca^{2+} imaging and a minimum of 15 cells and eight independent experiments for mitochondrial Ca^{2+} imaging. Individual cell recordings (gray) and average (black) were shown. ***G***, ***H***, Cytosolic ATP levels after a switch from HCSS medium to isosmotic KCl medium in which 30 mM NaCl was replaced by 30 mM KCl either in 2 mM Ca^{2+} medium or 100 μM EGTA medium. ***I***, Comparison between the two conditions. The drop in ATP values 200 s after isosmotic KCl stimulation was 18.6 ± 0.3% and 9 ± 0.1% with respect to basal levels in the presence and absence of Ca^{2+}, respectively ($^{**}p = 0.009$ two-tailed unpaired Student's *t* test). ***J–L***, Respiratory profiles, stimulation of mitochondrial respiration, and RCRs of neurons stimulated with hyperosmotic KCl in 2 mM Ca^{2+}, Ca^{2+}-free medium or 50 μM BAPTA preloaded neurons in 2 mM Ca^{2+}. ***M–O***, Corresponding data from neurons stimulated with isosmotic KCl using 10 μM BAPTA. RCR in nonstimulated state are represented with horizontal lines for each experimental condition ($n = 8$–30 experiments in *aralar* WT neuronal cultures; one-way ANOVA, $^{*}p \leq 0.05$, $^{***}p \leq 0.001$, *post hoc* Bonferroni test). ***P***, Changes in $[Na^{+}]_i$, in SBFI loaded neurons exposed to 5.4 or 30 mM isosmotic KCl in 2 mM Ca^{2+} or 100 μM EGTA medium as indicated. Monensin (Monen; 10 μM) and Ouabain (Oua; 0.1 mM) were added for equilibration of extra- and intracellular $[Na^{+}]$ at the end of the experiments. Individual cell recordings (gray) and average (black) were shown ($n = 29$).

lower than that caused by high K^{+} or veratridine. Carbachol specifically increased oligomycin sensitive respiration from 74.48 ± 1.97% to 84.38 ± 2.21 in basal and carcachol-induced OCR, respectively.

The role of Ca^{2+}-regulation of OCR with respect to ATP demand in the response to carbachol was evaluated by studying carbachol-stimulation of OCR in the presence of Ca^{2+} in BAPTA-AM loaded neurons, in which carbachol-induced Ca^{2+} transients were abolished (Fig. 6*C*), whereas store-operated Ca^{2+} entry is maintained or increased by preventing its Ca^{2+}-dependent inactivation (Litjens et al., 2004), a situation entailing conservation or even increase of workload in the absence of Ca^{2+} signaling. After BAPTA loading, carbachol-stimulation of OCR was halved (Fig. 6*G–I*), indicating that Ca^{2+} signaling to mitochondria is required to induce the full response to carbachol. Moreover, as the workload and ATP demand may be larger in BAPTA-loaded than control neurons, the real effect of Ca^{2+} on carbachol stimulation of OCR is probably underestimated.

Figure 7*A–C* shows that the lack of SCaMC-3 had no effect on carbachol-induced stimulation of OCR. However, ARALAR de-

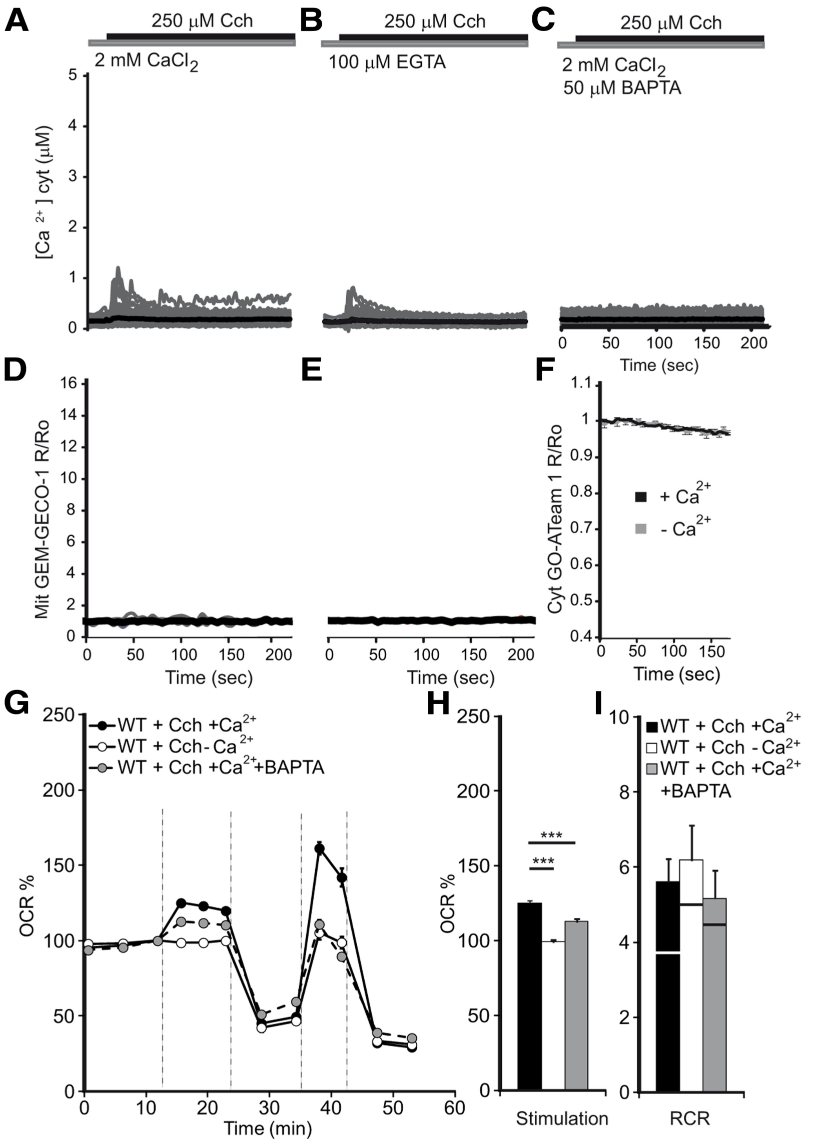

Figure 6. Changes in cytosolic and mitochondrial Ca^{2+}, cytosolic ATP and oxygen consumption in response to carbachol. ***A–C***, Changes in $[Ca^{2+}]_{cyt}$, in Fura-2-loaded neurons obtained by stimulation with 250 μM Carbachol (Cch) in 2 mM Ca^{2+}, Ca^{2+}-free medium, or 50 μM BAPTA preloaded neurons in 2 mM Ca^{2+} medium. ***D***, ***E***, Corresponding data in neurons transfected with Mit-GEM-GECO1 to determine changes in $[Ca^{2+}]_{mit}$. Recordings from at least 60 cells per condition and two independent experiments were used for cytosolic Ca^{2+} and a minimum of 15 cells and eight independent experiments for mitochondrial Ca^{2+}. Individual cell recordings (gray) and average (black) were shown. ***F***, Corresponding data for cytosolic ATP in neurons transfected with cyt-GO-ATeam1. Drop in ATP values 200 s after carbachol addition were 4.9 ± 0.8% and 2.1 ± 0.4% with respect to basal levels in the presence or absence of Ca^{2+} ($p = 0.92$, two-tailed unpaired Student's *t* test). ***G–I***, Respiratory profiles, stimulation of mitochondrial respiration, and RCRs of neurons stimulated with 250 μM carbachol in 2 mM Ca^{2+}, Ca^{2+}-free medium, or 50 μM BAPTA preloaded neurons in 2 mM Ca^{2+}. RCR in nonstimulated state were represented with horizontal lines for each experimental condition. Data from 18 to 22 experiments in *aralar* WT cultures (one-way ANOVA, $^{***}p \leq 0.001$, *post hoc* Bonferroni test).

ficiency resulted in a smaller stimulation in the presence of Ca^{2+} (Fig. 7*D–F*) suggesting that under this condition activation of the ARALAR-MAS pathway is required. The lack of ARALAR reflects a limitation in substrate supply to mitochondria, as pyruvate addition abolished the differences in carbachol-stimulation of OCR between ARALAR-deficient and WT neurons (Fig. 7*G–I*).

The requirement of ARALAR-MAS for the full respiratory response to carbachol in the presence of Ca^{2+} is possibly mediated through Ca^{2+}-activation of ARALAR in the intermembrane space rather than through changes in matrix Ca^{2+}, as no changes in mitochondrial Ca^{2+} were observed in response to carbachol, whereas high K^+ and veratridine caused rapid increases in mitochondrial Ca^{2+} in the presence, but not absence, of extracellular Ca^{2+}. The effect of BAPTA on carbachol stimulation of OCR is probably related to its effects in blunting the increase in cytosolic Ca^{2+} required to activate ARALAR-MAS at the mitochondrial intermembrane space.

Discussion

The role of Ca^{2+} in tuning ATP production to ATP demand in excitable cells has been known for a long time (Jouaville et al., 1999; Hayakawa et al., 2005; Glancy and Balaban, 2012; Rizzuto et al., 2012). However, in intact neurons the contribution of Ca^{2+} in adjusting coupled respiration to ATP demand is still controversial (Hayakawa et al., 2005; Mathiesen et al., 2011). A confounding variable in these studies is the fact that any increase in cytosolic Ca^{2+}, either by uptake from the extracellular space or release from intracellular Ca^{2+} stores, is necessarily coupled to the use of ATP to restore resting Ca^{2+} levels.

We have now addressed the following fundamental issues: (1) Are any of the brain Ca^{2+}-regulated mitochondrial carriers ARALAR or SCaMC-3 required in basal or maximal respiration of intact neurons using physiological glucose concentrations? (2) Is Ca^{2+} signaling (independently of Ca^{2+}-dependent increase in ATP demand) required to upregulate respiration in response to an increase in workload in intact neurons? (3) Are ARALAR or SCaMC-3 limiting such a Ca^{2+}-dependent upregulation of respiration?

We have first shown that mitochondrial respiration in nonstimulated intact cortical neurons using physiological glucose concentrations 2.5–5 mM (Lewis et al., 1974) depends on ARALAR-MAS, but not on SCaMC-3, and is reduced by 46% in neurons lacking ARALAR. This clearly indicates a most important role of ARALAR-MAS in shuttling NADH to mitochondria and providing pyruvate supply to the organelle. The lack of effect of external Ca^{2+} and exogenous pyruvate in basal respiration confirms that the main factor governing basal OCR is workload, i.e., ATP utilization (Brand and Nicholls, 2011).

We next analyzed the effects of different workloads on OCR under conditions in which Ca^{2+} signaling was allowed or prevented. These were provided by veratridine, high K^+-depolarization, and carbachol. In the presence of Ca^{2+}, veratridine causes an increase in cytosolic Ca^{2+} and Na^+ concentrations of 2–3 μM (Fig. 2) and 25 mM (Rose and Ransom, 1997), respectively. As estimated by Attwell and Laughlin (2001), any increase in $[Ca^{2+}]_{cyt}$ from 100 nM to 2–3 μM, in which 39 of every 40 Ca^{2+} atoms are buffered (Helmchen et al., 1997), would result in a net increase in ATP consumption of ~0.1 nM ATP in 1 μl cell volume to extrude

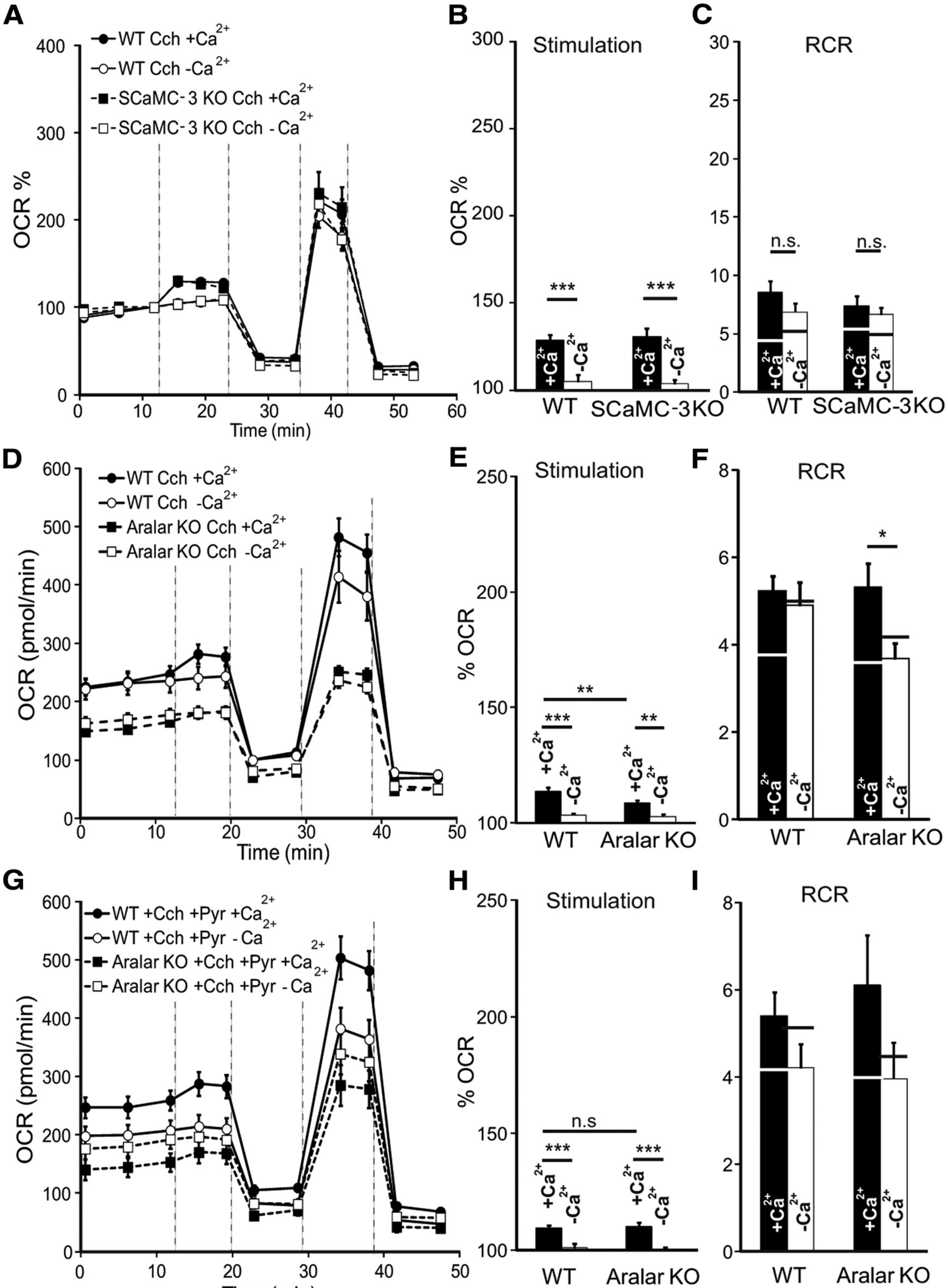

Figure 7. OCR response to Carbachol (Cch) in ARALAR- and SCaMC-3-deficient neuronal cultures. ***A–D***, Respiratory profiles in the presence or absence of 2 mM Ca^{2+}, stimulation of mitochondrial respiration, and RCRs of *SCaMC-3*-WT and *SCaMC-3*-KO neurons stimulated with 250 μM carbachol in 2.5 mM glucose. ***E–H***, Corresponding data from *aralar* WT and *aralar* KO neurons. ***G–I***, Corresponding data of the effect of 2 mM pyruvate (Pyr) on carbachol-induced mitochondrial respiration in *aralar* WT and *aralar* KO neurons. RCR in nonstimulated state are represented with horizontal lines for each experimental condition. Data from 5 to 6 experiments in *SCaMC-3*-WT and *SCaMC-3*-KO cultures, and from 4 to 12 experiments in *aralar* WT and *aralar* KO cultures (two-way ANOVA, $*p \leq 0.05$; $**p \leq 0.01$; $***p \leq 0.001$, *post hoc* Bonferroni test).

Ca^{2+} at a cost of 1 ATP/Ca^{2+} by plasma membrane or ER ATPases, and a demand of ~8.3 nM ATP to extrude Na^+ at a cost of 1 ATP/3 Na^+ through the Na^+, K^+-ATPase, i.e., a total demand of ~8.4 nM ATP, most of which are used for Na^+ extrusion. In other words, even if the $[Ca^{2+}]_{bound}/[Ca^{2+}]_{free}$ ratio may be higher (Martinez-Serrano et al., 1992), most of the ATP demand is due to Na^+ entry. Thirty millimoles of K^+ causes a nondetectable increase in $[Na^+]_i$ and an increase in $[Ca^{2+}]_i$, of 1–2 μM (Fig. 4), resulting in total ATP de-

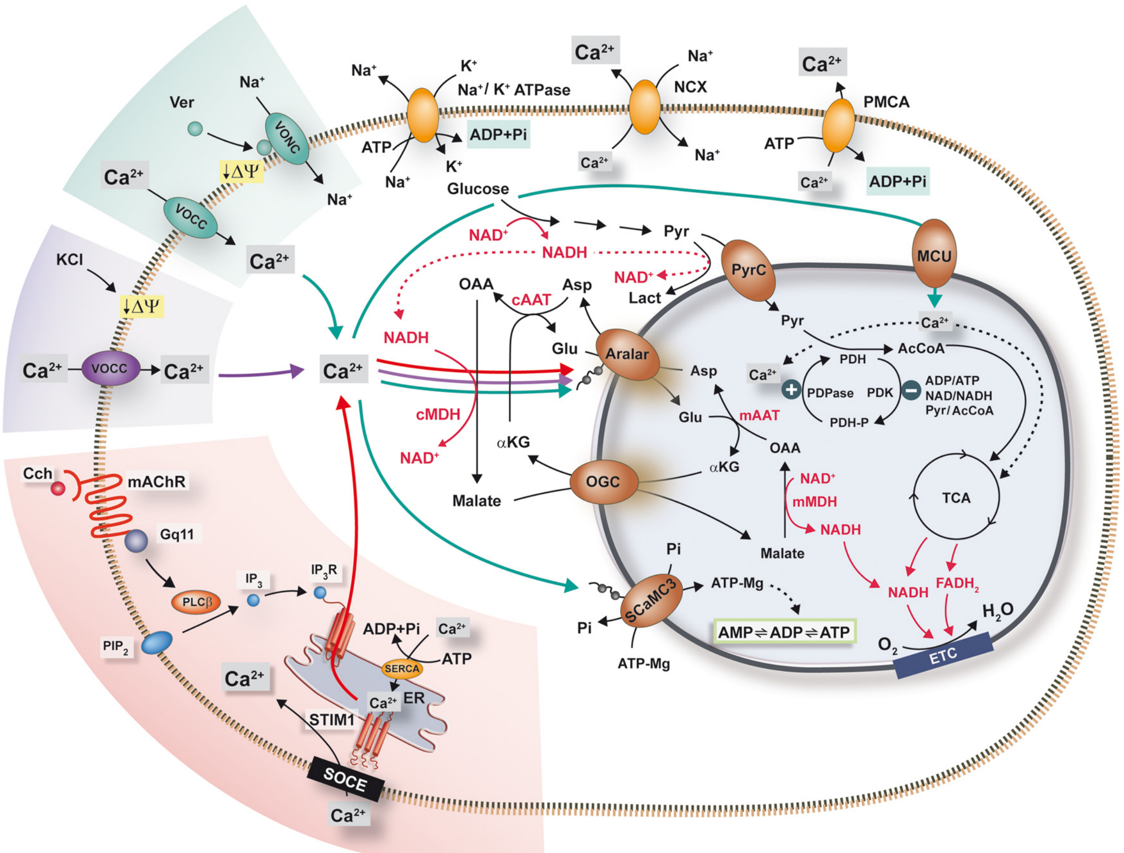

Figure 8. Schematic representation of the effects of the different workloads on Ca^{2+} regulation of neuronal oxygen consumption. Pathways indicated in green, purple, and red are activated by Veratridine (Ver), KCl, and Carbachol (Cch), respectively. All three stimuli activate ARALAR-MAS, increasing pyruvate supply in mitochondria, whereas only veratridine activates adenine nucleotide uptake through *SCaMC-3*. Veratridine also stimulates respiration after mitochondrial Ca^{2+} uptake through the MCU and activation of mitochondrial dehydrogenases. SOCE, Store operated Ca^{2+} entry; ETC, electron transport chain; AAT,aspartate aminotranferase; AcCoA, acetyl coenzyme A; Asp, aspartate; Cch, carbachol; ER, endoplasmic reticulum; ETC, electron transport chain; Glu, glutamate; IP_3, inositol trisphosphate; IP_3R, inositol 3-phosphate receptor; α-KG, α-ketoglutarate; mAChR, muscarinic cholinergic G-protein-coupled receptor; MCU, mitochondrial calcium uniporter; MDH, malate dehydrogenase; NCX, sodium calcium exchanger; OAA, oxaloacetate; OGC, oxoglutarate carrier; PDH, pyruvate dehydrogenase; PDKase, pyruvate dehydrogenase kinase; PDPase, pyruvate dehydrogenase phosphatase; PIP_2, phosphatidylinositol 4,5-bisphosphate; PLC-β, phospholipase C-β; PMCA, plasma membrane calcium ATPase; PyrC, pyruvate carrier; SERCA, sarco/endoplasmic reticulum Ca^{2+}-ATPase; SOCE, store-operated calcium entry; TCA, tricarboxylic acid cycle; Ver, veratridine; VOCC, voltage operated calcium channel; VONC, voltage operated sodium channel.

mand of ~0.06–0.08 nM per microliter of cell volume. For carbachol, with mean increases in $[Ca^{2+}]_i$ of ~0.1–0.2 μM, ATP demand is only due to Ca^{2+} extrusion and corresponds to ~0.01 nM ATP in 1 μl cell volume. In the presence of Ca^{2+}, the response to all three conditions was an immediate increase in oligomycin-sensitive OCR which persisted (KCl and carbachol) or declined (veratridine) during the following minutes.

In all cases the OCR response was severely reduced in the absence of Ca^{2+}, a condition that substantially lowers ATP demand in response to KCl and carbachol, but has a much smaller impact on workload in the case of veratridine, suggesting that lack of Ca^{2+}-regulation rather than lower ATP demand is responsible for the reduced veratridine-stimulation of OCR. Indeed, the decrease in cytosolic ATP levels caused by veratridine is more severe in Ca^{2+}-free media (Fig. 2) indicating that decreased mitochondrial production of ATP, not lower ATP demand, explains the neuronal response to this workload in Ca^{2+}-free medium. All stimuli caused a substantially lower increase in OCR in BAPTA-loaded neurons, in which workload is preserved, clearly indicating that Ca^{2+}-regulation of respiration is required to meet workload demands with an increase in OCR.

We next analyzed the mechanisms responsible for Ca^{2+}-regulation of respiration in the different workloads. For veratridine, the mechanism involved is clearly dependent on MCU as respiration in *aralar* KO neurons still responds to veratridine in a Ca^{2+}-dependent way (Fig. 3*G*). In these neurons, Ca^{2+} entry in mitochondria and activation of dehydrogenases together with activation of SCaMC-3 provide the only pathways of Ca^{2+}-regulation of mitochondrial respiration. As the blunted response to veratridine in *aralar* KO neurons is reversed by pyruvate supply both in the absence and presence of Ca^{2+} (Fig. 3), the results suggest that the increase in mitochondrial Ca^{2+} is insufficient to fully increase respiration upon veratridine challenge and MAS activity to push pyruvate in mitochondria (Gellerich et al., 2009) is clearly required.

On the other hand, the requirement of SCaMC-3 is different, as it is strictly Ca^{2+}-dependent. Isolated brain mitochondria from *SCaMC-3* mice exchange $[ATP\text{-}Mg]^{2-}$ or $[ADPH]^{2-}$ against P_i^{2-} across the inner mitochondrial membrane with an $S_{0.5}$ for Ca^{2+} activation of 3–4 μM within the same range of the MCU (Amigo et al., 2013). The uptake of adenine nucleotides stimulated by a large rise in cytosolic Ca^{2+} may affect mitochondrial function in two ways: by mass action ratio effects on the ATP synthase, causing an increase in coupled respiration as is thought to occur in hepatocytes (Aprille, 1988), or by increasing the Ca^{2+} retention capacity of mitochondria exposed to high Ca^{2+} loads

(Amigo et al., 2013). Further work is required to clarify the mechanism involved.

Ca^{2+}-regulation of OCR in response to KCl does not require SCaMC-3 but is absolutely dependent on ARALAR-MAS, as no increase in OCR was obtained in *aralar* KO neurons, whereas exogenous pyruvate allowed restoration of stimulated respiration to control values. As $[Ca^{2+}]_{mit}$ increases in this condition (Fig. 4*D*) regardless of ARALAR deficiency (Pardo et al., 2006), these results indicate that $[Ca^{2+}]_{mit}$ by itself is unable to increase respiration in response to this workload. In these conditions, $[Ca^{2+}]_{cyt}$ activation of ARALAR-MAS appears as the only pathway for Ca^{2+}-regulation of respiration in cortical neurons by "pushing" pyruvate into mitochondria, in other words, through an increase in pyruvate transport into mitochondria caused by an increase in cytosolic pyruvate. It is surprising that the increase in $[Ca^{2+}]_{mit}$ is not sufficient to activate pyruvate dehydrogenase (PDH) and other mitochondrial dehydrogenases and thereby "pull" pyruvate into mitochondria as occurs in *aralar* KO neurons stimulated by veratridine (pyruvate is expected to be pulled into mitochondria through the consumption of pyruvate by PDH and mass action ratio effects on the pyruvate carrier). Activation of PDH may require not only Ca^{2+}-activation of PDH phosphatase but inhibition of PDH kinases (PDKs) which inactivate PDH, through increases in mitochondrial pyruvate/acetyl-CoA and ADP/ATP ratios (Stacpoole, 2012). The high workload induced by veratridine, but not by KCl, associated with a more pronounced increase in mitochondrial ADP/ATP ratio may limit inhibition of PDKs and explain the lack of KCl-stimulated respiration in *aralar* KO neurons. On the other hand, whether ARALAR-MAS activity is also required to prime mitochondria for Ca^{2+} stimulation of metabolism is an open question.

Neurons respond to the small workload imposed by carbachol with a modest but sustained increase in OCR. Interestingly, the lack of ARALAR caused a significant decrease in this response in the presence, but not absence, of Ca^{2+}, suggesting that Ca^{2+}-activation ARALAR-MAS is the push mechanism to drive pyruvate in mitochondria upon carbachol exposure. The prominent role of ARALAR-MAS in regulating neuronal respiration in this condition agrees with the small size of the Ca^{2+} transient and lack of $[Ca^{2+}]_{mit}$ changes caused by carbachol (Fig. 6) and higher affinity of the ARALAR-MAS pathway than MCU for Ca^{2+} (300 nM vs a few μM), and with the finding of an essential role of AGC1-MAS in increasing mitochondrial NAD(P)H in response to small Ca^{2+} signals (Pardo et al., 2006).

Together, these results underscore the roles of MCU-$[Ca^{2+}]_{mit}$, ARALAR-MAS, and SCaMC-3 in upregulating oligomycin-sensitive respiration in cerebral cortex neurons in response to workloads produced by increases in Na^{+} and/or Ca^{2+} and robust-to-small Ca^{2+} signals (Fig. 8). These roles may vary in neurons from the adult brain due to changes in enzyme and transporter composition.

MCU-$[Ca^{2+}]_{mit}$ play a prominent role in the response to the large workload produced by veratridine. The ARALAR-MAS pathway also contributes in the regulation of pyruvate supply to mitochondria in this condition, greatly amplifying the OCR response. The ARALAR-MAS pathway plays an outstanding role in the response to smaller workloads, being the only Ca^{2+}-regulation mechanism responsible for upregulation of respiration in response to the small Ca^{2+} signals produced by carbachol. Surprisingly, it appears to be also the main mechanism responsible for Ca^{2+}-regulation of respiration in response to KCl, which induces large Ca^{2+} signals in mitochondria. In all cases, ARALAR-MAS through the Ca^{2+}-activation of ARALAR in the intermembrane space provides pyruvate to mitochondria. The mitochondrial ATP-Mg/Pi carrier SCaMC-3 limits respiration only in response to high workloads and robust Ca^{2+} signals which are able to activate carrier activity, as produced by veratridine, suggesting a requirement of adenine nucleotide uptake in mitochondria to generate a full respiratory response under these conditions.

References

Abramov AY, Duchen MR (2008) Mechanisms underlying the loss of mitochondrial membrane potential in glutamate excitotoxicity. Biochim Biophys Acta 1777:953–964. CrossRef Medline

Adler EM, Augustine GJ, Duffy SN, Charlton MP (1991) Alien intracellular calcium chelators attenuate neurotransmitter release at the squid giant synapse. J Neurosci 11:1496–1507. Medline

Álvarez G, Ramos M, Ruiz F, Satrústegui J, Bogónez E (2003) Pyruvate protection against β-amyloid-induced neuronal death: role of mitochondrial redox state. J Neurosci Res 73:260–269. CrossRef Medline

Amigo I, Traba J, González-Barroso MM, Rueda CB, Fernández M, Rial E, Sánchez A, Satrústegui J, Del Arco A (2013) Glucagon regulation of oxidative phosphorylation requires an increase in matrix adenine nucleotide content through Ca^{2+}-activation of the mitochondrial ATP-mg/pi carrier SCaMC-3. J Biol Chem 288:7791–7802. CrossRef Medline

Aprille JR (1988) Regulation of the mitochondrial adenine nucleotide pool size in liver: mechanism and metabolic role. FASEB J 2:2547–2556. Medline

Aprille JR, Rohweder-Dunn G, Brennan WA Jr, Kelley RT, Nosek MT (1987) Mitochondrial function after acute alteration of the endogenous insulin-to-glucagon ratio. Biochem Biophys Res Commun 142:315–321. CrossRef Medline

Ashton AC, Ushkaryov YA (2005) Properties of synaptic vesicle pools in mature central nerve terminals. J Biol Chem 280:37278–37288. CrossRef Medline

Asimakis GK, Aprille JR (1980) In vitro alteration of the size of the liver mitochondrial adenine nucleotide pool: correlation with respiratory functions. Arch Biochem Biophys 203:307–316. CrossRef Medline

Attwell D, Laughlin SB (2001) An energy budget for signaling in the grey matter of the brain. J Cereb Blood Flow Metab 21:1133–1145. CrossRef Medline

Bak LK, Obel LF, Walls AB, Schousboe A, Faek SA, Jajo FS, Waagepetersen HS. (2012) Novel model of neuronal bioenergetics: postsynaptic utilization of glucose but not lactate correlates positively with Ca^{2+} signalling in cultured mouse glutamatergic neurons. ASN Neuro 4:e00083. CrossRef Medline

Balaban RS (2009) The role of Ca(2+) signaling in the coordination of mitochondrial ATP production with cardiac work. Biochim Biophys Acta 1787:1334–1341. CrossRef Medline

Baughman JM, Perocchi F, Girgis HS, Plovanich M, Belcher-Timme CA, Sancak Y, Bao XR, Strittmatter L, Goldberger O, Bogorad RL, Koteliansky V, Mootha VK (2011) Integrative genomics identifies MCU as an essential component of the mitochondrial calcium uniporter. Nature 476:341–345. CrossRef Medline

Brand MD, Nicholls DG (2011) Assessing mitochondrial dysfunction in cells. Biochem J 435:297–312. CrossRef Medline

Cárdenas C, Miller RA, Smith I, Bui T, Molgó J, Müller M, Vais H, Cheung KH, Yang J, Parker I, Thompson CB, Birnbaum MJ, Hallows KR, Foskett JK (2010) Essential regulation of cell bioenergetics by constitutive InsP3 receptor Ca^{2+} transfer to mitochondria. Cell 142:270–283. CrossRef Medline

Cerdan S, Künnecke B, Seelig J (1990) Cerebral metabolism of [1,2-$^{13}C_2$] acetate as detected by in vivo and in vitro ^{13}C NMR. J Biol Chem 265: 12916–12926. Medline

Chouhan AK, Ivannikov MV, Lu Z, Sugimori M, Llinas RR, Macleod GT (2012) Cytosolic calcium coordinates mitochondrial energy metabolism with presynaptic activity. J Neurosci 32:1233–1243. CrossRef Medline

Courtney MJ, Lambert JJ, Nicholls DG (1990) The interactions between plasma membrane depolarization and glutamate receptor activation in the regulation of cytoplasmic free calcium in cultured cerebellar granule cells. J Neurosci 10:3873–3879. Medline

Cuezva JM, Burkett ES, Kerr DS, Rodman HM, Patel MS (1982) The new-born of diabetic rat: 1. hormonal and metabolic changes in the postnatal period. Pediatr Res 16:632–637. CrossRef Medline

del Arco A, Satrústegui J (1998) Molecular cloning of Aralar, a new member of the mitochondrial carrier superfamily that binds calcium and is present in human muscle and brain. J Biol Chem 273:23327–23334. CrossRef Medline

del Arco A, Satrústegui J (2004) Identification of a novel human subfamily of mitochondrial carriers with calcium-binding domains. J Biol Chem 279:24701–24713. CrossRef Medline

De Stefani D, Raffaello A, Teardo E, Szabò I, Rizzuto R (2011) A forty-kilodalton protein of the inner membrane is the mitochondrial calcium uniporter. Nature 476:336–340. CrossRef Medline

Drago I, Pizzo P, Pozzan T (2011) After a century mitochondrial in- and efflux machineries reveal themselves. EMBO J 30:4119–4125. CrossRef Medline

Fiermonte G, De Leonardis F, Todisco S, Palmieri L, Lasorsa FM, Palmieri F (2004) Identification of the mitochondrial ATP-mg/pi transporter: bacterial expression, reconstitution, functional characterization, and tissue distribution. J Biol Chem 279:30722–30730. CrossRef Medline

Gellerich FN, Gizatullina Z, Arandarcikaite O, Jerzembek D, Vielhaber S, Seppet E, Striggow F (2009) Extramitochondrial Ca^{2+} in the nanomolar range regulates glutamate-dependent oxidative phosphorylation on demand. PLoS One 4:e8181. CrossRef Medline

Gellerich FN, Gizatullina Z, Trumbekaite S, Korzeniewski B, Gaynutdinov T, Seppet E, Vielhaber S, Heinze HJ, Striggow F (2012) Cytosolic Ca^{2+} regulates the energization of isolated brain mitochondria by formation of pyruvate through the malate-aspartate shuttle. Biochem J 443:747–755. CrossRef Medline

Gellerich FN, Gizatullina Z, Gainutdinov T, Muth K, Seppet E, Orynbayeva Z, Vielhaber S (2013) The control of brain mitochondrial energization by cytosolic calcium: the mitochondrial gas pedal. IUBMB Life 65:180–190. CrossRef Medline

Glancy B, Balaban RS (2012) Role of mitochondrial Ca^{2+} in the regulation of cellular energetics. Biochemistry 51:2959–2973. CrossRef Medline

Grossbard L, Schimke RT (1966) Multiple hexokinases of rat tissues: purification and comparison of soluble forms. J Biol Chem 241:3546–3560. Medline

Grynkiewicz G, Poenie M, Tsien RY (1985) A new generation of Ca^{2+} indicators with greatly improved fluorescence properties. J Biol Chem 260: 3440–3450. Medline

Hayakawa Y, Nemoto T, Iino M, Kasai H (2005) Rapid Ca^{2+}-dependent increase in oxygen consumption by mitochondria in single mammalian central neurons. Cell Calcium 37:359–370. CrossRef Medline

Helmchen F, Borst JG, Sakmann B (1997) Calcium dynamics associated with a single action potential in a CNS presynaptic terminal. Biophys J 72:1458–1471. CrossRef Medline

Jalil MA, Begum L, Contreras L, Pardo B, Iijima M, Li MX, Ramos M, Marmol P, Horiuchi M, Shimotsu K, Nakagawa S, Okubo A, Sameshima M, Isashiki Y, del Arco A, Kobayashi K, Satrústegui J, Saheki T (2005) Reduced *N*-acetylaspartate levels in mice lacking Aralar, a brain- and muscle-type mitochondrial aspartate-glutamate carrier. J Biol Chem 280:31333–31339. CrossRef Medline

Jouaville LS, Pinton P, Bastianutto C, Rutter GA, Rizzuto R (1999) Regulation of mitochondrial ATP synthesis by calcium: evidence for a long-term metabolic priming. Proc Natl Acad Sci U S A 96:13807–13812. CrossRef Medline

Kelly JF, Furukawa K, Barger SW, Rengen MR, Mark RJ, Blanc EM, Roth GS, Mattson MP (1996) Amyloid beta-peptide disrupts carbachol-induced muscarinic cholinergic signal transduction in cortical neurons. Proc Natl Acad Sci U S A 93:6753–6758. CrossRef Medline

Kipanyula MJ, Contreras L, Zampese E, Lazzari C, Wong AK, Pizzo P, Fasolato C, Pozzan T (2012) Ca^{2+} dysregulation in neurons from transgenic mice expressing mutant presenilin 2. Aging Cell 11:885–893. CrossRef Medline

Lewis LD, Ljunggren B, Norberg K, Siesj ö BK (1974) Changes in carbohydrate substrates, amino acids and ammona in the brain during insulin-induced hypoglycemia. J Neurochem 23:659–671. CrossRef Medline

Litjens T, Harland ML, Roberts ML, Barritt GJ, Rychkov GY (2004) Fast-Ca^{2+}-dependent inactivation of the store-operated Ca^{2+} current (ISOC) in liver cells: a role for calmodulin. J Physiol 558:85–97. CrossRef Medline

Lucas-Meunier E, Fossier P, Baux G, Amar M (2003) Cholinergic modulation of the cortical neuronal network. Pflugers Arch 446:17–29. Medline

Mallilankaraman K, Cárdenas C, Doonan PJ, Chandramoorthy HC, Irrinki KM, Golenár T, Csordás G, Madireddi P, Yang J, Müller M, Miller R, Kolesar JE, Molgó J, Kaufman B, Hajnóczky G, Foskett JK, Madesh M (2012a) MCUR1 is an essential component of mitochondrial Ca^{2+} uptake that regulates cellular metabolism. Nat Cell Biol 14:1336–1343. CrossRef Medline

Mallilankaraman K, Doonan P, Cárdenas C, Chandramoorthy HC, Müller M, Miller R, Hoffman NE, Gandhirajan RK, Molgó J, Birnbaum MJ, Rothberg BS, Mak DO, Foskett JK, Madesh M (2012b) MICU1 is an essential gatekeeper for MCU-mediated mitochondrial Ca(2+) uptake that regulates cell survival. Cell 151:630–644. CrossRef Medline

Martinez-Serrano A, Blanco P, Satrústegui J (1992) Calcium binding to the cytosol and calcium extrusion mechanisms in intact synaptosomes and their alterations with aging. J Biol Chem 267:4672–4679. Medline

Mathiesen C, Caesar K, Thomsen K, Hoogland TM, Witgen BM, Brazhe A, Lauritzen M (2011) Activity-dependent increase in local oxygen consumption correlate with postsynaptic currents in the mouse cerebellum in vivo. J Neurosci 31:18327–18337. CrossRef Medline

McCormack JG, Halestrap AP, Denton RM (1990) Role of calcium ions in regulation of mammalian intramitochondrial metabolism. Physiol Rev 70:391–425. Medline

Mitchell P, Moyle J (1969) Estimation of membrane potential and pH difference across the cristae membrane of rat liver mitochondria. Eur J Biochem 7:471–484. Medline

Nakano M, Imamura H, Nagai T, Noji H (2011) Ca^{2+} regulation of mitochondrial ATP synthesis visualized at the single cell level. ACS Chem Biol 15:709–715. CrossRef Medline

Nicholls DG (2005) Mitochondria and calcium signaling. Cell Calcium 38: 311–317. CrossRef Medline

Palmieri L, Pardo B, Lasorsa FM, del Arco A, Kobayashi K, Iijima M, Runswick MJ, Walker JE, Saheki T, Satrústegui J, Palmieri F (2001) Citrin and aralar1 are Ca^{2+}-stimulated aspartate/glutamate transporters in mitochondria. EMBO J 20:5060–5069. CrossRef Medline

Pardo B, Contreras L, Serrano A, Ramos M, Kobayashi K, Iijima M, Saheki T, Satrústegui J (2006) Essential role of Aralar in the transduction of small Ca^{2+} signals to neuronal mitochondria. J Biol Chem 281:1039–1047. CrossRef Medline

Pardo B, Rodrigues TB, Contreras L, Garzón M, Llorente-Folch I, Kobayashi K, Saheki T, Cerdan S, Satrústegui J (2011) Brain glutamine synthesis requires neuronal-born aspartate as amino donor for glial glutamate formation. J Cereb Blood Flow Metab 31:90–101. CrossRef Medline

Putney JW (2009) Capacitative calcium entry: from concept to molecules. Immunol Rev 231:10–22. CrossRef Medline

Qian W, Van Houten B (2010) Alterations in bioenergetics due to changes in mitochondrial DNA copy number. Methods 51:452–457. CrossRef Medline

Ramos M, del Arco A, Pardo B, Martínez-Serrano A, Martínez-Morales JR, Kobayashi K, Yasuda T, Bogónez E, Bovolenta P, Saheki T, Satrústegui J (2003) Developmental changes in the Ca^{2+}-regulated mitochondrial aspartate-glutamate carrier aralar1 in brain and prominent expression in the spinal cord. Brain Res Dev Brain Res 143:33–46. CrossRef Medline

Rego AC, Ward MW, Nicholls DG (2001) Mitochondria control AMPA/kainate receptor-induced cytoplasmic calcium deregulation in rat cerebellar granule cells. J Neurosci 21:1893–1901. Medline

Rizzuto R, De Stefani D, Raffaello A, Mammucari C (2012) Mitochondria as sensors and regulators of calcium signalling. Nat Rev Mol Cell Biol 13: 566–578. CrossRef Medline

Rose CR, Ransom BR (1997) Regulation of intracellular sodium in cultured rat hippocampal neurones. J Physiol 499:573–587. Medline

Ruiz F, Álvarez G, Pereira R, Hernández H, Villalba M, Cruz F, Cerdán S, Bogónez E, Satrústegui J (1998) Protection by piruvate and malate against glutamate-mediated excitotoxicity. Neuroreport 9:1277–1282. Medline

Sánchez-Cenizo L, Formentini L, Aldea M, Ortega AD, García-Huerta P, Sánchez-Aragó M, Cuezva JM (2010) Up-regulaton of the ATPase inhibitory factor 1 (IF1) of the mitochondrial H+-ATP synthase in human tumors mediates the metabolis shift of cancer cells to a Warburg phenotype. J Biol Chem 285:25308–25313. CrossRef Medline

Satrústegui J, Pardo B, del Arco A (2007) Mitochondrial transporters as novel targets for intracellular calcium signaling. Physiol Rev 87:29–67. CrossRef Medline

Stacpoole PW (2012) The pyruvate dehydrogenase complex as a therapeutic target for age-related diseases. Aging Cell 11:371–377. CrossRef Medline

Strichartz G, Rando T, Wang GK (1987) An integrated view of the molecular toxinology of sodium channel gating in excitable cells. Annu Rev Neurosci 10:237–267. CrossRef Medline

Traba J, del Arco A, Duchen MR, Szabadkai G, Satrústegui J (2012) SCaMC-1 promotes cancer cell survival by desensitizing mitochondrial permeability transition via ATP/ADP-mediated matrix Ca(2+) buffering. Cell Death Differ 19:650–660. CrossRef Medline

Zhao Y, Araki S, Wu J, Teramoto T, Chang YF, Nakano M, Abdelfattah AS, Fujiwara M, Ishihara T, Nagai T, Campbell RE (2011) An expanded palette of genetically encoded Ca^{2+} indicators. Science 333:1888–1891. CrossRef Medline